Spring 2015

Computational valve plate design

Paul K. Kalbfleisch
Purdue University

Graduate School Form 30
Updated 1/15/2015

PURDUE UNIVERSITY
GRADUATE SCHOOL
Thesis/Dissertation Acceptance

This is to certify that the thesis/dissertation prepared

By Paul K Kalbfleisch

Entitled
COMPUTATIONAL VALVE PLATE DESIGN

For the degree of Master of Science in Engineering

Is approved by the final examining committee:

Monika Ivantysynova
Chair

Stuart Bolton

Charles Krousgrill

To the best of my knowledge and as understood by the student in the Thesis/Dissertation Agreement, Publication Delay, and Certification Disclaimer (Graduate School Form 32), this thesis/dissertation adheres to the provisions of Purdue University's "Policy of Integrity in Research" and the use of copyright material.

Approved by Major Professor(s): Monika Invantysynova

Approved by: Ganesh Subbarayan 4/16/2015
Head of the Departmental Graduate Program Date

COMPUTATIONAL VALVE PLATE DESIGN

A Thesis
Submitted to the Faculty
of
Purdue University
by
Paul Kalbfleisch

In Partial Fulfillment of the
Requirements for the Degree
of
Master of Science in Engineering

May 2015
Purdue University
West Lafayette, Indiana

To my family

ACKNOWLEDGEMENTS

First and foremost, I would like to thank my major advisor Professor Monika Ivantysynova for your continuing support and encouragement throughout the course of my research at the Maha Fluid Power Research Center. Your honest investment in my success has been a tremendous inspiration to my continuing development in both professional and personal components of my life.

I would also like to thank my advising committee members, Professor Stuart Bolton and Professor Charles Krousgrill for your knowledge and expertise. Thank you for your contribution to educating students at Purdue University.

I am grateful for my fellow researchers, past and present, which have helped me along the way. I thank Ganesh and Dongjune for their previous research and contributions to the field of valve plate optimization. I am thankful for Taeho Kim for working alongside me on valve plate research and for listening to all my ramblings of ideas and brainstorming. I am frankly beholden to Andrew Schenk for his generous guidance and help in programming C++, parallelism, and optimization knowledge.

My motivation in the lab could not have been possible without the help and support of my family and friends. I would first like to thank Doctor Ajita Narayan for your excellent treatment of my life and health. I would like to thank my family, Mom, Dad, Rachael, Andrew, Adam and Samantha for encouraging me and having faith in me. Last, but certainly not least, I would like to thank my girlfriend Autumn for your love and support through my rambles about work and being patient with me when I'm stuck inside my headspace.

TABLE OF CONTENTS

Page

LIST OF TABLES

LIST OF FIGURES

Figure Page

NOMENCLATURE

Symbol	Description	Units
A	Area	[m^2]
A_{rHP}	Valve plate area open to discharge port	[m^2]
A_{rLP}	Valve plate area open to suction port	[m^2]
A_k	Piston Area	[m^2]
a_k	Piston Acceleration	[m/s^2]
D_{DCFV}	diameter of DCFV port	[m]
D_{PCFV}	diameter of PCFV port	[m]
d_K	Piston diameter	[m]
F	Force	[N]
H_K	Piston stroke	[m]
i	Axial index	[-]
K	Fluid Bulk modulus	[Pa]
M_x	Swash plate moment about X axis	[Nm]
M_y	Swash plate moment about Y axis	[Nm]
M_z	Swash plate moment about Z axis	[Nm]
n	Rotational speed	[rpm]
p	Pressure	[Pa]
p_i	i^{th} displacement chamber pressure	[Pa]
p_{DC}	Displacement chamber pressure	[bar]
Δp	Pressure differential	[bar]
Q	Flow rate	[m^3/s]
Q_e	Effective flow rate	[m^3/s]
Q_{geo}	Geometric flow rate	[m^3/s]

Symbol	Description	Units
Q_{kin}	Kinematic flow rate	[m^3/s]
Q_s	Volumetric loss flow rate	[m^3/s]
Q_{sB}	Gap flow through VP and CB	[m^3/s]
Q_{se}	Volumetric flow through lubricating interfaces	[m^3/s]
Q_{sG}	Gap flow through slipper and swash plate	[m^3/s]
Q_{si}	Internal volumetric losses	[m^3/s]
Q_{sk}	Gap flow through piston and cylinder block	[m^3/s]
R_b	Cylinder block pitch radius	[m]
s_K	Piston stroke	[m]
t	Time	[s]
V	Displacement chamber volume	[m^3]
V_i	Derived displacement volume	[m^3]
V_{dead}	Displacement volume dead volume	[m^3]
v_k	Piston velocity	[m/s]
z_k	Number of pistons	[-]
$\overline{\boldsymbol{x}}$	Design Vector	[-]
α_D	Orifice coefficient of discharge	[-]
β	Swash plate angle	[°]
ΔM_x	Amplitude of swash plate moment M_x	[Nm]
ΔM_y	Amplitude of swash plate moment M_y	[Nm]
ΔM_z	Amplitude of swash plate moment M_z	[Nm]
ΔQ_{HP}	Amplitude of swash plate moment Q_{HP}	[L/min]
η_v	Volumetric efficiency	[-]
ρ	Oil density	[kg/m^3]
σ	Contact stress	[Pa]
φ	Shaft angular position	[°]
ω	Angular velocity	[rad/s]
ϕ	Piston angular position	[rad]

LIST OF ABBREVIATIONS

Abbreviation	Description
ABN	Airborne Noise
AVAS	Automated Valve plate Area Search
CFD	Computational Fluid Dynamics
CW	Clock Wise
DC	Displacement Chamber
FBNS	Fluid Borne Noise Source
HP	High Pressure
IDC	Inner Dead Center
LP	Low pressure
LSODA	Livermore Solver of Differential equations Automatic
ODC	Outer Dead Center
OPCON	Operating Condition
SBNS	Structure Borne Noise Source
Vol Eff*	Volumetric Efficiency (without external leakages)
VP	Valve plate
VpOptim	Valve Plate Optimization
WCF	Windows Communication Framework
Δ	Change

ABSTRACT

Kalbfleisch, Paul. M.S.E., Purdue University, May 2015. Computational Valve Plate Design. Major Professor: Monika Ivantysynova, School of Mechanical Engineering.

Axial piston machines are widely used in many industries for their designs compactness, flexibility in power transfer, variable flow rate, and high efficiencies as compared to their manufacturing costs. One important component of all axial piston machines that is a very influential on the performance of the unit is the valve plate. The aim of this research is to develop a design methodology that is general enough to design all types of valve plates and the simple enough not to require advanced technical knowledge from the user. A new style of valve plate designs has been developed that comprehensively considers all previous design techniques and does not require significant changes to the manufacturing processes of valve plates. The design methodology utilizes a previously developed accurate computer model of the physical phenomenon. This allows the precise optimization of the valve plate design through the use of simulations rather than expensive trial and error processes. The design of the valve plate is clarified into the form of an optimization problem. This formulation into an optimization problem has motivated the selection of an optimization algorithm that satisfies the requirements of the design. The proposed design methodology was successfully tested in a case study in the shown to be very successful in improving required performance of the valve plate design.

CHAPTER 1. INTRODUCTION

1.1 Background

Fluid power, also known as hydraulics, the technology used in a wide variety of applications such as construction machines, aerospace, automotive, offshore, medical devices, material handling, agricultural and for street machinery, manufacturing, robots, railways. The main component of any fluid power system is the use of a category of pumps and motors referred to as positive displacement machines. There are several types of positive displacement machines including axial piston type, radial piston type, gear type, and screw type.

One very popular group of positive displacement machines are the axial piston machines. Like any positive displacement machine, axial piston machines are designed to displace fluid in order to transfer power in order to do useful work. Axial piston machines are widely used in many industries for their designs compactness, flexibility in power transfer, variable flow rate, and high efficiencies as compared to their manufacturing costs. They are also attractive due to their ability to operate as a pump or motor. Negatively, they are also known for their high audible noise levels.

Recent trends of hydraulic systems are towards more efficient systems and higher performance especially through increase of operating pressures. The replacement of valve controlled systems through displacement control actuation introduces different new challenges in pump and motor design, which also affects the valve plate design. Also, as variable displacement pumps and motors are used as the heart of the hydraulic hybrid systems, these units are forced to work under more varying operating conditions (speed, displacement, and working pressure). This increases the difficulty for the design of the valve plate as the valve plate's influence on the pump is dependent on the operating conditions. These advancements enable fluid power systems to become more efficient,

compact, and power dense. The design of a valve plate is an extremely important part of the design of an axial piston machine.

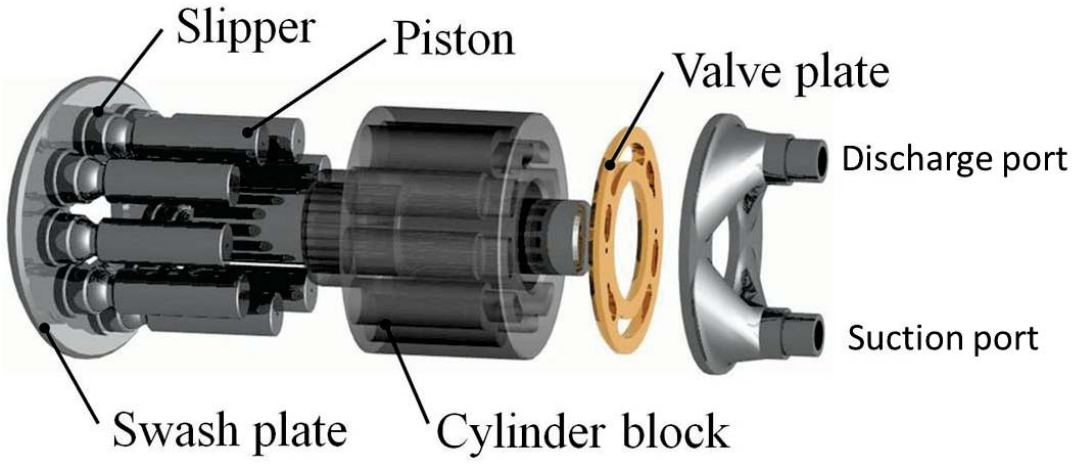

Figure 1.1. Axial piston machine.

The basic operation of a piston pump involves the motion of a discrete number of pistons, each displacing a certain amount of fluid (displacement volume) as the piston moves from its outer dead center to its inner dead center, i.e. while decreases the displacement. As shown in Figure 1.2, in swashplate type axial piston machines the pistons are supported on the swash plate, the cylinder block usually rotates while the swash plate is stationary. The valve plate connects the individual cylinder bores with the pump/motor high pressure and low pressure (suction in case of pump operation) port. The cylinder bore is also called displacement chamber, as it defines how much fluid can be displaced by each piston over one shaft revolution.

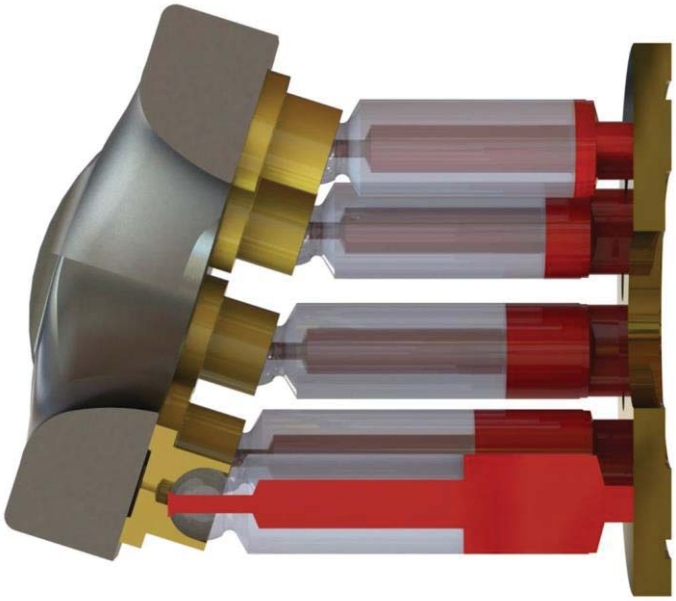

Figure 1.2. Displacement chambers.

As each displacement chamber rotates around the shaft, the valve plate is connects the displacement chamber to the suction port or to the discharge port, or to both. Consequently, the valve plate design defines the time of connection of each displacement chamber to the pump/motor high pressure and low pressure port. In order to achieve a certain timing relief grooves are often introduced, which will influence when a certain displacement chamber with respect to its piston position is opened to suction or high pressure port. This opening/closing will influence the pressure build up in each displacement chamber, which will strongly influence the pump/motor operation.

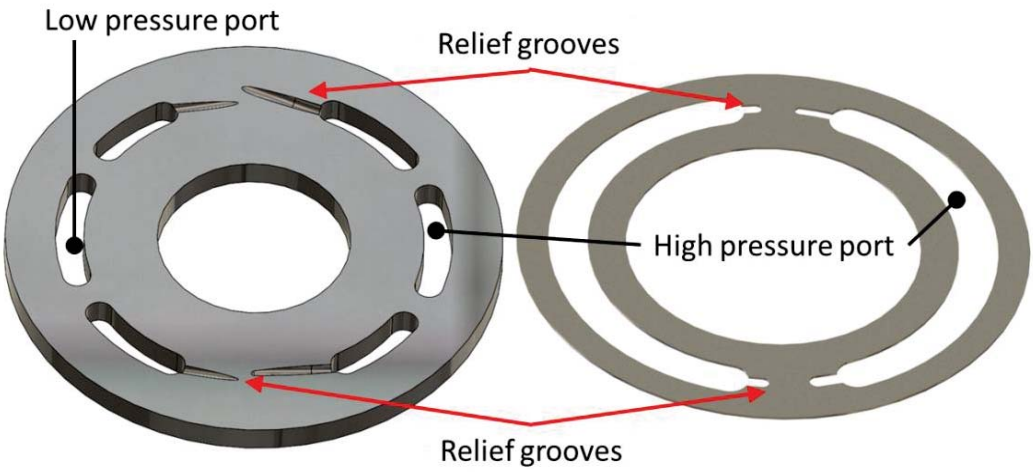

Figure 1.3. Valve plate examples.

Figure 1.3 shows an example of two different types of valve plate designs, a thick valve plate and a valve plate. The aim of this thesis is to propose a computational based design methodology to optimize the valve plate design with respect to the pump/motor performance and noise emissions. In addition to the timing of the connection of the displacement chamber with the pump/motor ports, the valve plate/cylinder block interface acts on a seal and a thrust bearing. In order to fulfill this sealing and bearing function a sealing land has to be connected on the valve plate or the cylinder block surface around the opening of the valve plate in order to seal the high pressure of fluid film formed on the sealing land area between the valve plate and the cylinder block will help to separate the valve plate surface from the rotating cylinder block bottom surface and with that prevent high motion and wear. The hydrostatic and hydrodynamic pressure built up in the fluid film creates the required load carrying ability of the film and simultaneously seals the high pressure port through a controlled leakage. The amount of leakage and load carrying ability is controlled by the sealing land design. This part of valve plate design is not part of this research. The focus of the design optimization of the valve plate investigated within this thesis is the timing of the displacement chamber connection to the pump/motor ports.

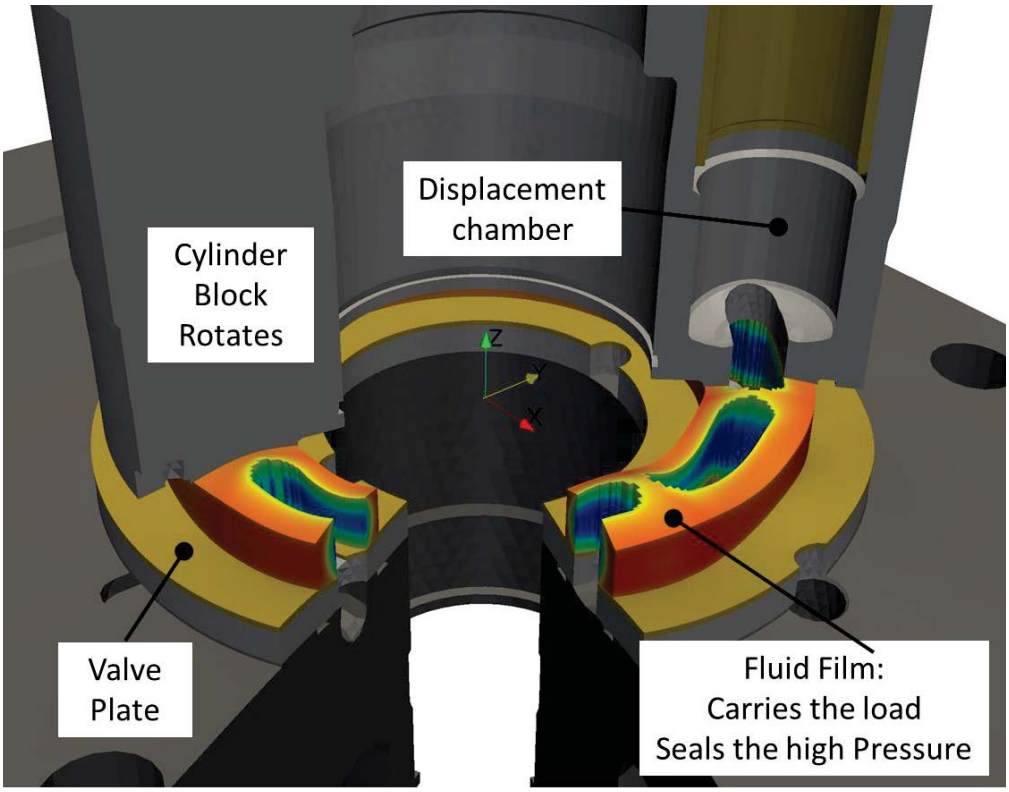

Figure 1.4. Cylinder block/valve plate interface (Zecchi, 2013).

This gap between the cylinder block and valve plate must maintain a micrometers thick film of fluid in order to lubricate the moving part. This lubricating gap has to fulfill simultaneously a bearing and sealing function under various dynamic loading conditions. The design of this lubricating interface is crucial to the operation of the pump, but will not be covered in this thesis. I referred the interested reader to the PhD disertation of (Zecchi, 2013) for the state of the art in cylinder block/valve plate interface modeling and design.

CHAPTER 2. STATE OF THE ART

2.1 State of the Art in Valve Plate Design

The motivation for the development of better valve plate designs has been predominantly focused on the reduction of structure borne noise sources (SBNS), and fluid borne noise sources (FBNS). Detailed summaries of the various noise reduction techniques can be found in Edge, 1999 and Seeniraj (2009). Though evolution of positive displacement machines has been shaped through tremendous progress, the problem of noise generation by pumps still remains a challenge.

Research in the area of noise reduction for axial piston pumps dates back to the early 1970s. One of the earliest works on hydraulic noise, Becker (1970) reported the effect of port timing (valve plate) on the displacement chamber pressure and pump outlet flow variations. This work on port timing establishes that rate of pressurization and pump noise are related. This work also correlated the frequency of noise generated with the number of displacement chambers and speed. Becker's work on port timing was later generalized in greater detail by Helgestad et al. (1974). That work presented effects of relief groove geometry and ideal timing on the rate of pressurization and excitation of pump casing. Yamauchi and Yamamoto (1976) publicized a study listing numerous factors (rate of pressurization, relief grooves, dead volume, speed, pressure, number of pistons, cavitation, and swash plate stiffness) that contributed to swash plate vibrations.

A major research project in fluid power noise reduction was started in 1976 in the United Kingdom funded by the government in which University of bath was involved. This project helped bring together different issues contributing to hydraulic noise (Edge, 1999), which led to many new reduction techniques and standards for quantifying noise.

Valve plate design was also considered for the reduction of fluid borne noise sources in the summary of reduction techniques and their limitations were completed by Harrison (1997) and Johansson (2005). The simplest reduction technique is ideal timing. Ideal timing is understood to be intentionally delaying the opening between the displacement chamber and each of the ports. However, using ideal timing to achieve compression is effective only for a particular pressure level and for fixed displacement pumps (Helgestad, 1974; Yamauchi and Yamamoto, 1976; Edge, 1989 and Pettersson, 1991). Relief grooves were found to be less sensitive to pressure levels and speeds than ideal timing. Also relief grooves spread out the compressibility effect (Pettersson et al., 1991 and Harrison, 1997). Relief grooves achieve compression using high pressure fluid from discharge port. Rate of compression is controlled by geometry of relief grooves limiting back flow from discharge port into displacement chamber (Palmberg, 1989). Achieving compression with fluid from discharge port creates a strong correlation between groove geometry and flow ripple. Also relief grooves have influence on the volumetric efficiency if there is cross porting between discharge and suction ports (Pettersson et al., 1991).

Design methodologies based on computational design have recently been developed following the enormous strides in the field of computer science (Seeniraj, 2009) and (Kim D. , 2012). These 2 design methodologies will be expanded upon in section **Error! Reference source not found.**

2.2 State of the Art in Optimization

The previous research conducted in the field of optimization is an enormous amount of literature to summarize. A brief summary of the general categories of optimization research will be presented, but will quickly proceed to the specific field of algorithms considered for the proposed design methodology. Current real-world problems in engineering, that require optimization, are considerably more complex for the classical (gradient-based) optimization algorithms to efficiently solve. The increase in complexity of engineering models, with the inclusion of numerical methods; make it very difficult and computational expensive to calculate the derivatives of the solution space. To circumvent the difficulties with gradient-based methods, research into heuristic

(experience based) methods were developed. The evolution of heuristic methods created a more general class of optimization algorithms referred to as metaheuristic algorithms.

2.2.1 Metaheuristic Optimization

Blum and Roli (2003) provide a detailed overview in comparison of the many different metaheuristic methods involved in combinatorial optimization. They quote Osman defining the general class of metaheuristics. "A metaheuristic is formally defined as an iterative generation process which guides a subordinate heuristic by combining intelligently different concepts for exploring and exploiting the search space, learning strategies are used to structure information in order to find efficiently near-optimal solutions (Osman, 1993)."

Blum and Roli (2003) list a few famous metaheuristic algorithms including (but not limited to): Ant Colony Optimization (ACO), Evolutionary algorithms (EA) including Genetic Algorithms (GA), Iterated Local Search (ILS), Simulated Annealing (SA), and Tabu Search (TS).

Figure 2.1 graphically characterizes many different popular metaheuristic algorithms. The most important category for consideration of valve plate design was the population-based algorithms. By far the most popular metaheuristic methods are those found within the category of evolutionary algorithms. Evolutionary algorithms have shown a tremendous rate of success when used to solve very complex optimization problems including: multi-objective, multimodal, nonlinear, heavily constrained, and globally optimal.

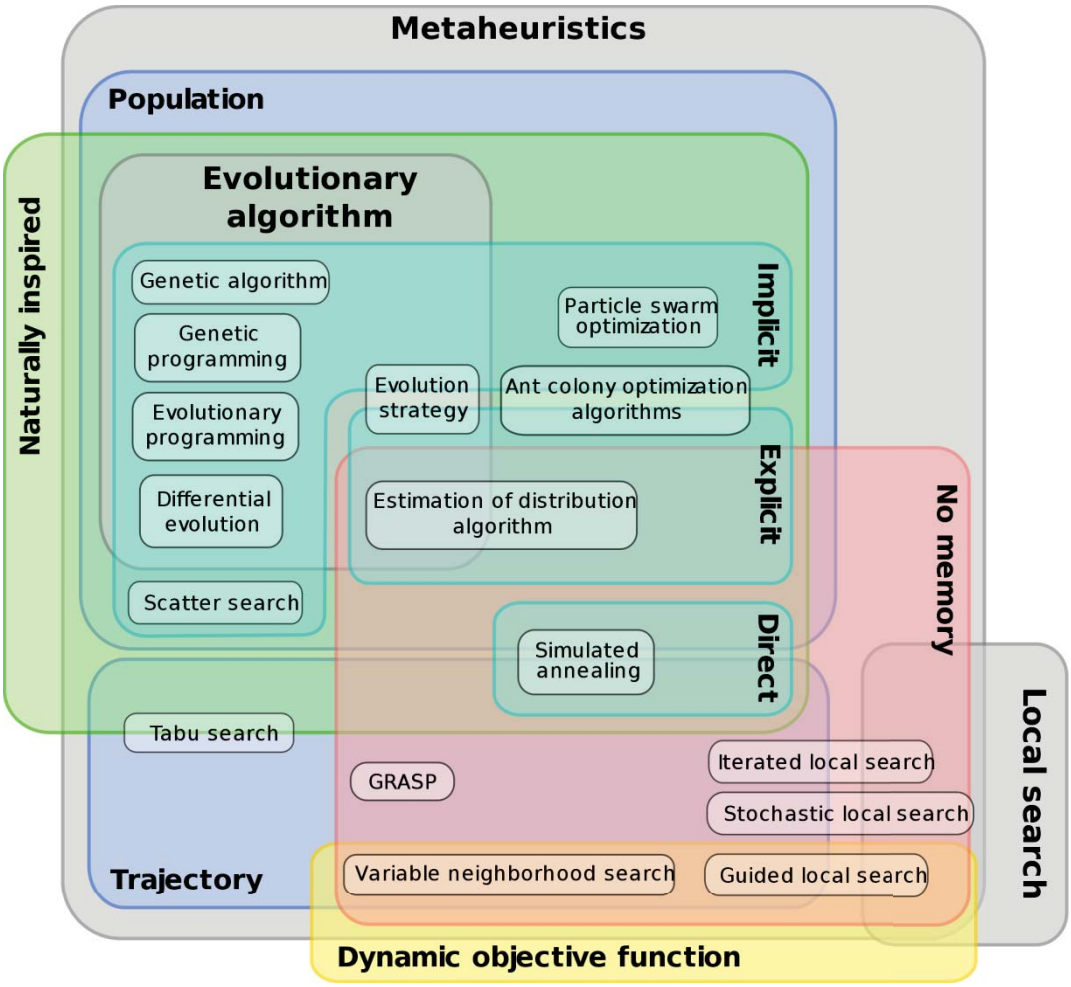

Figure 2.1. Metaheuristics classification (Dréo, 2007).

2.2.2 Evolutionary Algorithms

Tiwari et al. (2011) provides a very detailed literature review on the development of evolutionary algorithms ability solve multi-objective problems and multi-modal problems. Evolutionary algorithms are inspired from nature and the working principal is based on Darwin's theory of "Survival of the fittest" (Holland 1975, Dawkins 1976, Eldridge 1989). The robust and adaptive nature of EA's is exploited by design optimization through the use of variation operators and an appropriate fitness function.

The genetic algorithm (GA) (Goldberg, 1989)has been, by far, the most popular among the list of Evolutionary algorithms. A GA is usually population based (a set of solutions) instead of a single solution (individual). This property has made the GA very popular in the field of multi-objective optimization where the final solution is typically a

set of solutions (along the Pareto front). Ehrgott (2012) documents the history of Pareto Optimality. Vilfredo Pareto was known for being a great Italian economics, born in 1848, and developed the concept of Pareto optimal. Selection among the Pareto optimal designs requires the loss of one performance parameter in order to improve another. A very simple economic example involves deciding between quality and cost of a product. One most sacrifice cost in order to increase quality. A more precise definition is given in Ehrgott (2012). The population based approach of the GA makes it very resilient to early converge to a non-globally optimal solution. Tiwari et al. (2011) highlights developments in each of the 5 key concepts every multi-objective genetic algorithm must contain. The concepts are as follows: population approach, selection mechanism, diversity assessment, variation operators, and knowledge integration.

Two notable concepts that have great influence in the design of this thesis are the concepts of non-domination sorting (rank) (Deb, Pratap, Agarwal, & Meyarivan, 2002) and the crowding distance metrics (Deb, Pratap, Agarwal, & Meyarivan, 2002). The introduction in both of these concepts in the same article led me to later utilize the proposed algorithm (NSGA-II).

2.3 Previous Design of Experiments

Within the research group of Prof. Ivantysynova, there have been two researchers that have made contributions to the topic of valve plate design. As I've inherited their research contributions is important to understand the state-of-the-art on that topic within the Maha Fluid Power Research Center.

2.3.1 Ganesh Seeniraj, 2009

Seeniraj (2009) was the 1st to develop a design methodology for valve plates in swash plate type axial piston machines. Although great advances have been made upon his original design methodology is important to understand the fundamental design concepts he created. Convinced by Edge (1999), Seeniraj developed a design methodology to reduce both structure borne noise sources and fluid borne noise sources. This led Seeniraj to the field of multiobjective optimization. Multiobjective optimization

attempts to minimize multiple objective functions (performance parameters) simultaneously. There will be at some point a subjective decision made in order to choose the priority of the various objective functions.

Seeniraj (2009) was the 1st to parameterize the area files into several variables in order to systematically describe the geometry of the valve plate with a vector of numbers. His original valve plate Parameterization only included symmetric linear grooves. This terminology will be explained later, but is written here for the sake of clarity and completion.

Seeniraj (2009) also discovered that the performance of the valve plate is dependent on the various operating conditions. This led to the generalization that every objective function must be minimized, also at every operating condition (Opcon). The operating conditions are a continuous range and therefore it is impossible to simulate all of them. This led Seeniraj (2009) to the idea of sampling the Opcons in an intelligent way in order to estimate the entire operating condition range with only a few simulated points. Seeniraj (2009) chose the 8 corner points of the 3 variable (dimensions) operating condition space. At that time, Seeniraj did not have a clear understanding of what the operating condition space would look like and therefore chose the 8 extreme points for safety.

As later explained in Section 3.5, the numerical solver Seeniraj was using was considerably slower. This motivated Seeniraj to develop a constraint function. This constraint function would use in a nontraditional manner. The constraint function was used to reduce the amount of function evaluations done. This constraint is labeled in Figure 2.2. Seeniraj algorithm as “fitness evaluation”, but will later be referred to as the “peak test”. For safety, Seeniraj immediately discarded valve plate designs that had significant “over pressurization” or “cavitation” at the specified operating condition.

I disagree with Seeniraj’s classification of his algorithm as a “Multi-objective Optimization Genetic Algorithm (MOGA)”. I classify his optimization algorithm as an ineffective combination of a full factorial search and grid search. A true full factorial design of experiments does not require changing of the “parameter intervals”. Therefore, Seeniraj’s algorithm is hard to classify due to its unique design.

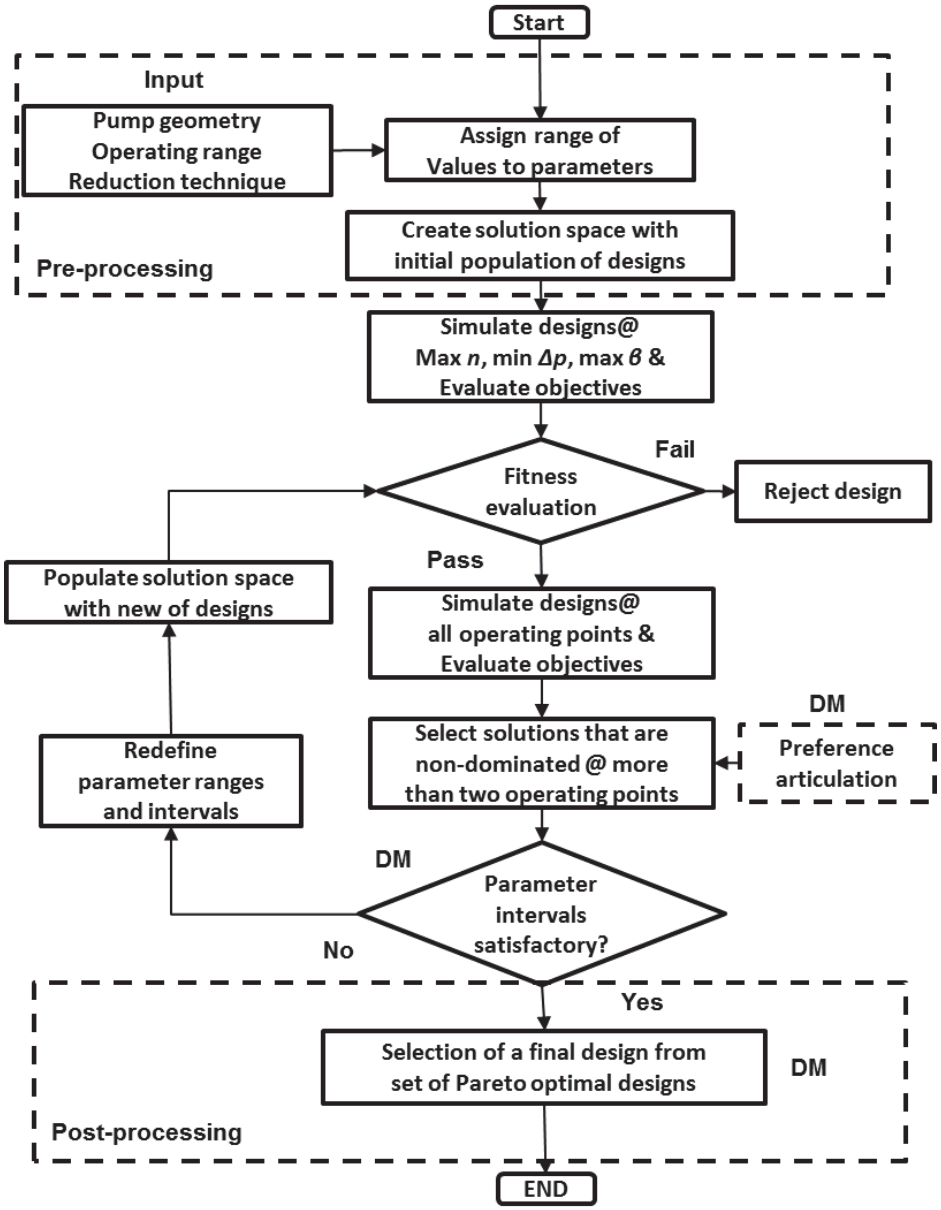

Figure 2.2. Seeniraj algorithm.

The most important fact to notice in Figure 2.2. Seeniraj algorithm is the letters “DM” written in various locations. These letters stand for “decision maker” and require the user of the algorithm to make a decision throughout the design process. The most crucial “DM” is located within a loop. This requires the user of the algorithm to be present at the computer/work for the algorithm to continue. This process and computer science is known as a barrier and requires the entire algorithm to become inefficient while waiting

for the input of the user. Upon testing, Seeniraj's algorithm, it became apparent that a lot of nights in weekend time was wasted due to this barrier. This barrier problem will be later fixed in CHAPTER 4.

2.3.2 Dongjune Kim, 2012

Kim's improvements to Seeniraj's original algorithm were incremental. Kim spent less time on valve plate design and therefore had much smaller contributions to the algorithm. The similarities of Kim's algorithm to Seeniraj's algorithm included: the peak test, slow design times, full factorial search, original valve plate needed, and "DM" with in the loop.

Kim's changes to Seeniraj's algorithm that were not kept in this thesis were as follows. Kim reduced the number of Opcons sampled to 3, but gave no explanation for the safety of that reduction. Kim solved the multi-objective problem by instituting a weighted average approach, but only did a single set of weights instead of the conventional range in order to build a Pareto front. Kim also normalized the different objective functions in order for his weights in the average to hold a significant meaning, but throughout the algorithm the normalized values would change, constantly altering the weights. This was not noticed by Kim, because his design of experiments was a single full factorial search around the original design. In the time between Kim and Seeniraj the widespread use of multicore computers was influential in Kim's algorithm to manually parallelize the computations on various computers. This also contributed to the variations in effective weights (within the weighted average) placed on the various computers. Therefore, the designs chosen from at the end of his algorithm were not comparable.

The improvement made by Kim (2012) that was kept was the addition of the volumetric efficiency check. However, the use of the volumetric efficiency check is fundamentally different than Kim (2012). Kim implemented the volumetric efficiency check in order to speed up the design process and/or reduce the amount of function evaluations. Kim's algorithm would 1st check the peak values in order to throw out designs followed by checking the volumetric efficiency to throw out designs (I, therefore, disagree with Kim's algorithm flow chart (Figure 2.3) with the implementation of the

volumetric efficiency check.) This method of excluding designs based on constraints had 2 main problems. First, the use of constraints to reduce function evaluations encourages the designer to heavily constrained the problem more than what is necessary for proper design only in order to save time. As can be seen in Kim's results (Kim D. , 2012), his final design had a high volumetric efficiency, but sacrificed on other objective functions. Secondly, while the original idea of: throwing out designs in order to run less simulations saves time seems correct on the surface, it did not. Because of the nature of the non-stiff solver, the volumetric efficiency check would require 15 minutes of simulation time, while the following simulations would only take on the order of 30 seconds. Therefore, Kim's volumetric efficiency test would spend 15 minutes trying to save 30 seconds. Upon testing of Kim's algorithm, the order was quickly reversed, and then later the volumetric efficiency test was removed until a new solver (LSODA Section 3.5) was implemented.

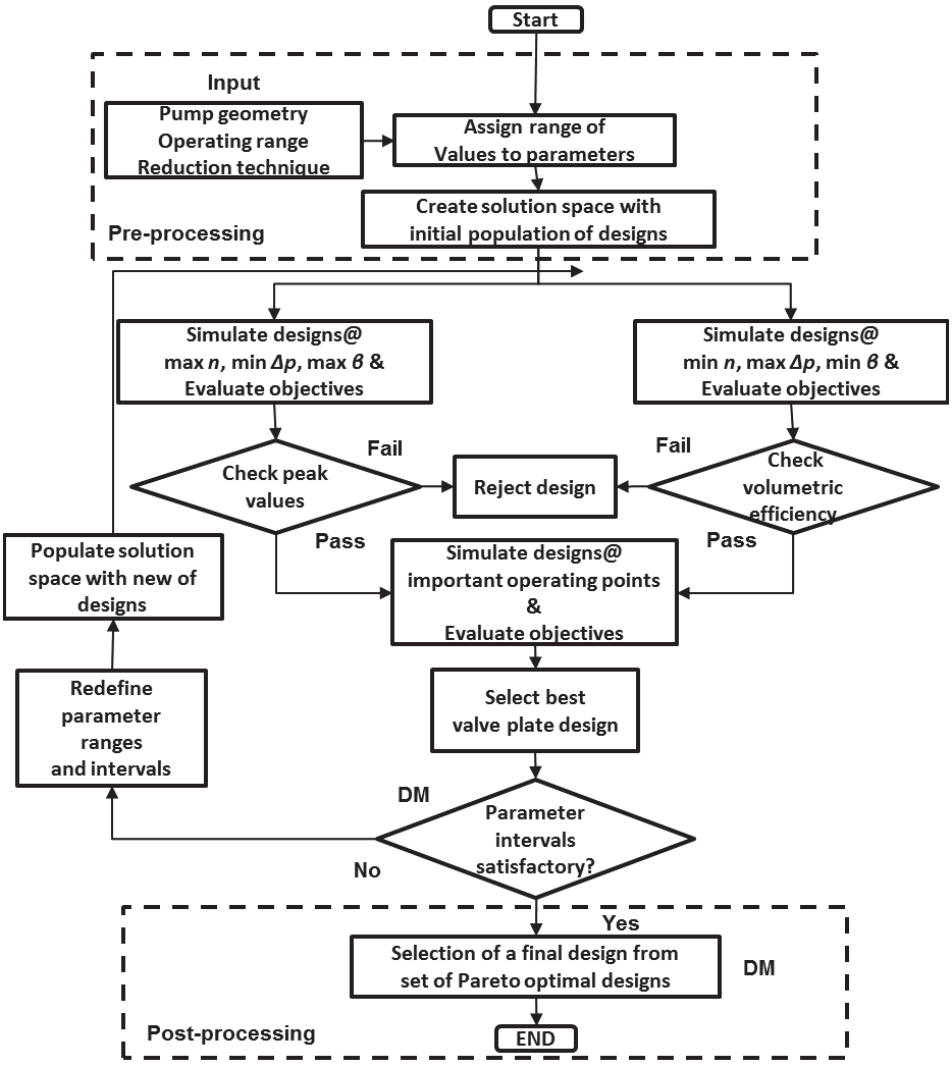

Figure 2.3. Kim Algorithm.

CHAPTER 3. COMPUTATIONAL MODEL

This chapter stands for the understanding of fundamentals that are essential to understand the valve plate design. The contents are referred from Ivantysyn and Ivantysynova (2001), and Wieczorek (2002).

3.1 The Swash Plate Type Axial Piston Machine

This chapter explains the working principle of a swash plate type piston machine and the physics that are involved in order to understand the axial piston machine behavior.

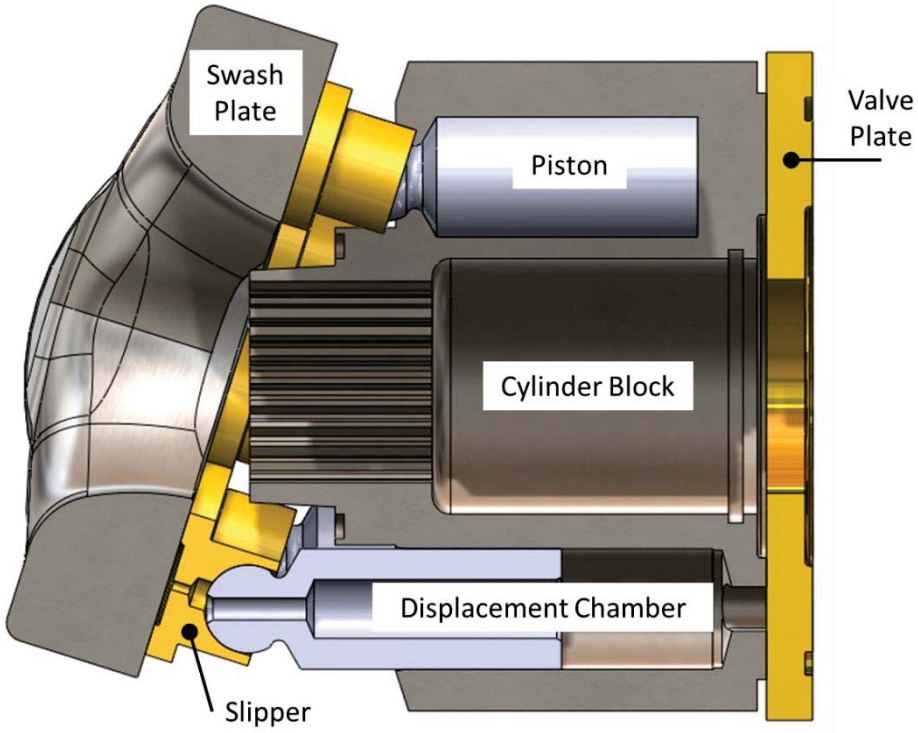

Figure 3.1. Swash plate type axial piston machine.

Figure 3.1. shows the rotating group of a swash plate type axial piston machine. The rotating group consists of three main rotating components: cylinder block, pistons, and slippers. The non-rotating parts are the valve plate and the swash plate.

In pumping mode of the swash plate type axial piston machine, the shaft is driven by an external power source and torque is transferred to the cylinder block. The cylinder block rotates with the shaft and pistons while valve plate and swash plate remains stationary. The stroke of the pistons depends on the angle of the swash plate. In motoring mode, the high pressure fluid enters displacement chamber in the cylinder block and moves the piston. And the piston side force is transferred to the cylinder block generating torque on the cylinder block that transferred to the shaft.

3.2 Swash Plate Type Piston Machine Kinematics

Figure 3.2. describes an axial piston machine with parameters related to the kinematics of an axial piston machine (Ivantysn & Ivantysynova, 2001). The coordinate system is also described in Figure 3.2. The swash plate rotates on the x-axis and the z-axis is parallel to the shaft. Thus the y-axis is defined by the right hand law.

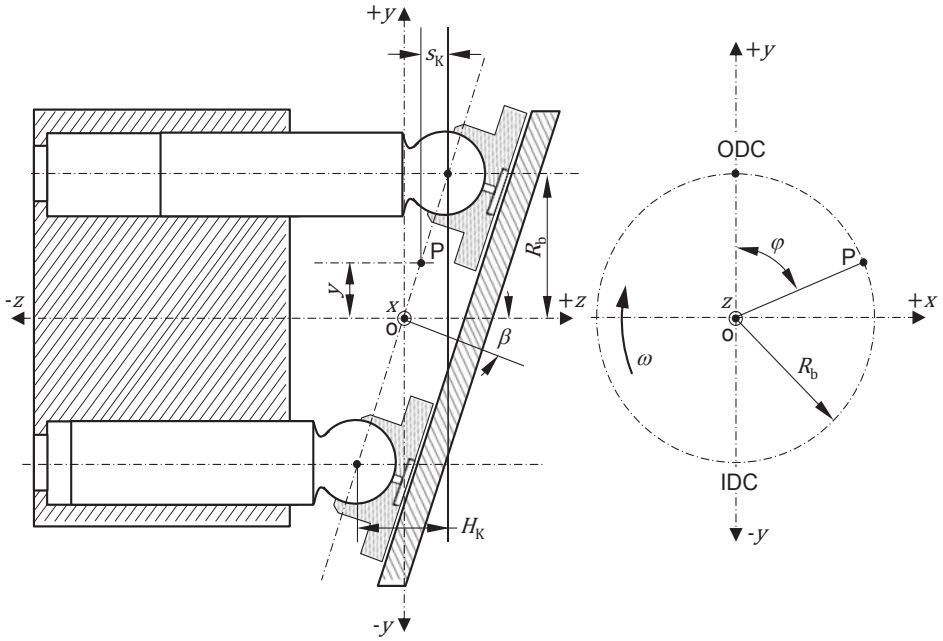

Figure 3.2. Schematic of a swash plate type axial piston machine (Ivantysn & Ivantysynova, 2001).

The shaft rotates on the z-axis with a constant angular rotational speed (ω) for all revolutions. The displacement of the piston (s_K) is in the z-axis direction,

$$s_K = -z\,. \tag{3.1}$$

The pitch radius (R_B) and angular position (ϕ) of the piston affect the displacement such that,

$$z = b \cdot tan\,\beta\,, \tag{3.2}$$

$$b = R_B - y\,, \tag{3.3}$$

and

$$y = R_B \cdot \cos\phi\,. \tag{3.4}$$

Therefore, the displacement of the piston (s_K) can be described as,

$$s_K = -R_B \cdot tan\,\beta \cdot (1 - cos\,\phi). \tag{3.5}$$

From this equation, we find that the maximum displacement is achieved at a half revolution when the piston is at ϕ = 180°, this location is referred to as the inner dead center (IDC). By similar derivation, the piston stroke (H_K) can be described as,

$$H_K = 2R_B \cdot \tan\beta\,. \tag{3.6}$$

Also, the relative velocity of the piston in z-axis is

$$v_K = \frac{ds_K}{dt} = \frac{ds_K}{d\phi} \cdot \frac{d\phi}{dt} = \frac{ds_K}{d\phi} \cdot \omega \tag{3.7}$$

when using the displacement of the piston (s_K) equation, which is

$$\frac{ds_K}{d\phi} = -R_B \cdot tan\,\beta \cdot sin\,\phi\,. \tag{3.8}$$

Substituting this equation to Eq. (3.7) leads to

$$v_K = -\omega \cdot R_B \cdot tan\,\beta \cdot sin\,\phi \tag{3.9}$$

which can also be expressed with the piston stroke as,

$$v_K = -\frac{1}{2} \cdot \omega \cdot H_K \cdot sin\,\phi\,. \tag{3.10}$$

Then the acceleration of the piston becomes

$$a_K = \frac{dv_K}{dt} = \frac{dv_K}{d\phi} \cdot \frac{d\phi}{dt} = \frac{dv_K}{d\phi} \cdot \omega\,. \tag{3.11}$$

Substituting each variable into this equation yields

$$a_K = -\omega^2 \cdot R_B \cdot tan\,\beta \cdot \cos\phi\,. \tag{3.12}$$

Similar to the relative velocity equation, this equation can be expressed by the piston stroke (H_K),

$$a_K = -\frac{1}{2} \cdot \omega^2 \cdot H_K \cdot sin\,\phi\,. \tag{3.13}$$

The circumferential velocity of the piston caused by the rotation of the cylinder block is

$$v_u = R_B \cdot \omega\,. \tag{3.14}$$

Thus the radial acceleration becomes

$$a_u = R_B \cdot \omega^2\,. \tag{3.15}$$

The volume in the displacement chamber is continuously changing due to the linear motion of the piston. The volume change rate in regards to the time is

$$\frac{dV_i}{dt} = v_K \cdot A_K\,. \tag{3.16}$$

The symbol A_K stands for the area of the piston. Now we can substitute v_K into the following equation,

$$\frac{dV_i}{dt} = -\omega \cdot R_B \cdot A_K \cdot tan\,\beta \cdot sin\,\phi\,. \tag{3.17}$$

Writing this equation with the piston stroke (H_K) yields

$$\frac{dV_i}{dt} = -\frac{1}{2} \cdot \omega \cdot A_K \cdot H_K \cdot sin\,\phi\,. \tag{3.18}$$

The definition of the displacement chamber volume is

$$V_i = V_0 - V = V_0 - s_K \cdot A_K = V_0 + R_B \cdot \tan\beta \cdot (1 - \cos\phi) \cdot A_K\,. \tag{3.19}$$

where the symbol V_0 stands for the volume at the piston position at ϕ = 0°. We call this specific position the outer dead center (ODC). The dead volume (V_{DEAD}) is the smallest achievable volume in the displacement chamber and it occurs at the IDC.

3.3 Displacement Chamber Pressure

Figure 3.3. is a schematic of the piston and displacement chamber. It shows the control volume chosen to calculate the instantaneous pressure in the displacement chamber.

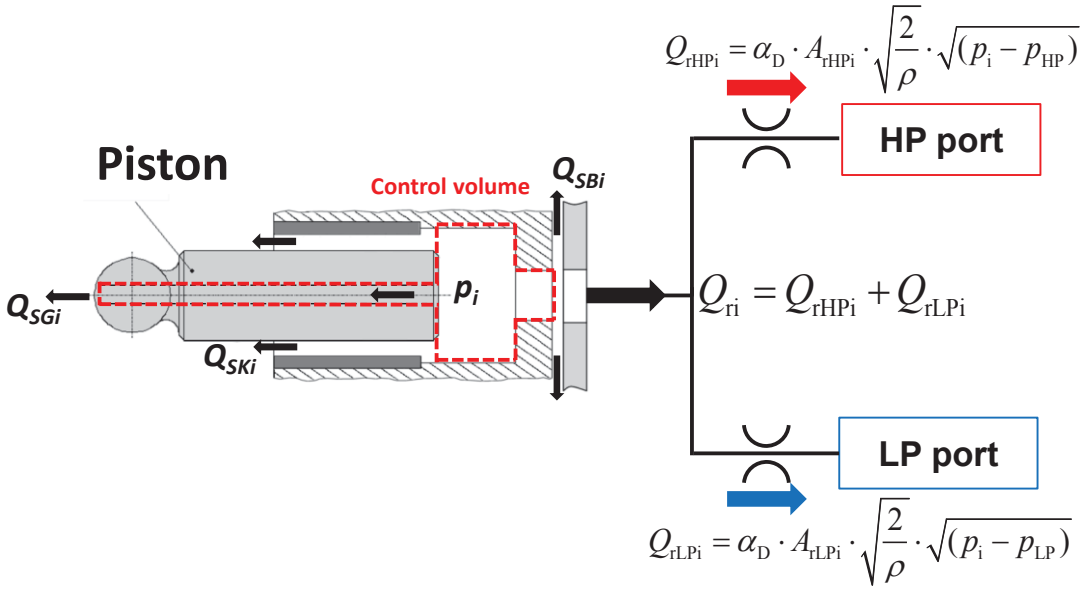

Figure 3.3. Control volume of displacement chamber (Kim, Kalbfleisch, & Ivantysynova, 2014).

The pump model simulates the individual flow of all the displacement chambers to and from both the HP port and LP port. The instantaneous displacement chamber pressure, within the pump model, is calculated in each displacement chamber using the pressure build up Eq. (3.20) by summing all the flows entering and exiting a control volume depicted in Figure 3.3

$$\frac{dp_i}{dt} = \frac{K}{V_i}\left(Q_{ri} - Q_{SKi} - Q_{SBi} - Q_{SGi} - \frac{dV_i}{dt}\right) \tag{3.20}$$

Q_{SKi} represents the leakage flow rate between each piston and cylinder. Q_{SBi} represents the leakage flow rate between the cylinder block and valve plate. Q_{SGi} represents the leakage flow rate through the piston bore to the slipper. Q_{SKi}, Q_{SBi}, and Q_{SGi} can be set to zero when neglecting the effect of external leakages. Qri represents the volumetric flow into a single displacement chamber and is calculated by summing the fluid flow between the displacement chamber and the each port, shown in Equation (3.20.

$$Q_{ri} = Q_{rHPi} + Q_{rLPi} \tag{3.21}$$

QrHPi represents the volumetric flow from a single displacement chamber to the HP port. QrLPi represents the flow to a single displacement chamber from the LP port as described in Figure 3.3. Both flows are assumed be turbulent and are modeled using the orifice equation. A positive flow represents fluid flowing into the displacement chamber, and a negative flow represents fluid flowing out of the displacement chamber.

$$Q_{rLPi} = \alpha_{DLP} \cdot A_{rLPi} \cdot \sqrt{\frac{2|p_i - p_{LP}|}{\rho}} sgn(p_i - p_{LP}) \tag{3.22}$$

and

$$Q_{rHPi} = \alpha_{DHP} \cdot A_{rHPi} \cdot \sqrt{\frac{2|p_i - p_{HP}|}{\rho}} sgn(p_i - p_{HP}) \tag{3.23}$$

A_{rLPi} and A_{rHPi} are incorporated into the model through the use of a predefined lookup table. This lookup table includes each an A_{rLPi} and A_{rHPi} for a set number of discrete time/phi steps. A_{rLPi} and A_{rHPi} are therefore defined as the minimum cross-sectional area perpendicular to a streamline at each angular position of the cylinder block for a single displacement chamber. The areas in between the table values are created by linear interpolating within the table. This table is external to the model, and is referred as an Area file. For an existing design, the area file is measured from the geometry of the pump. An additional software was developed using a given CAD geometry and computational fluid dynamics (CFD) to automatically calculate these areas. Figure 3.4. depicts an example of AVAS (Ivantysynova, Huang, & Christiansen, 2004) calculating a single streamline using CFD, and taking consecutive cross-sectional areas of the fluid volumes in order to find the smallest cross-sectional area. A close-up of the smallest cross-sectional area perpendicular to a streamline for the example angular position of the piston is shown below in Figure 3.4. (Right)

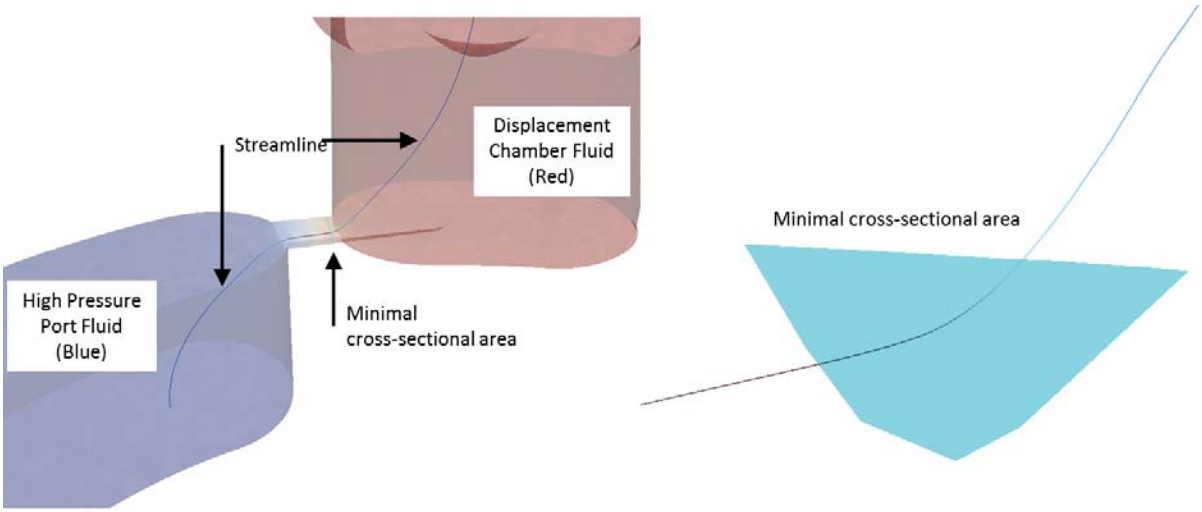

Figure 3.4. Calculated streamline (Left). Minimum opening area from displacement chamber to the port through the valve plate (Right).

Figure 3.4. only demonstrates the minimum cross-sectional area for a single port. In reality each displacement chamber could be connected to both ports of the pump at any given angular position (time). Therefore, the area file contains two areas for each angular position phi (ϕ). In arbitrary area file is graphed for a 44cc axial piston pump.

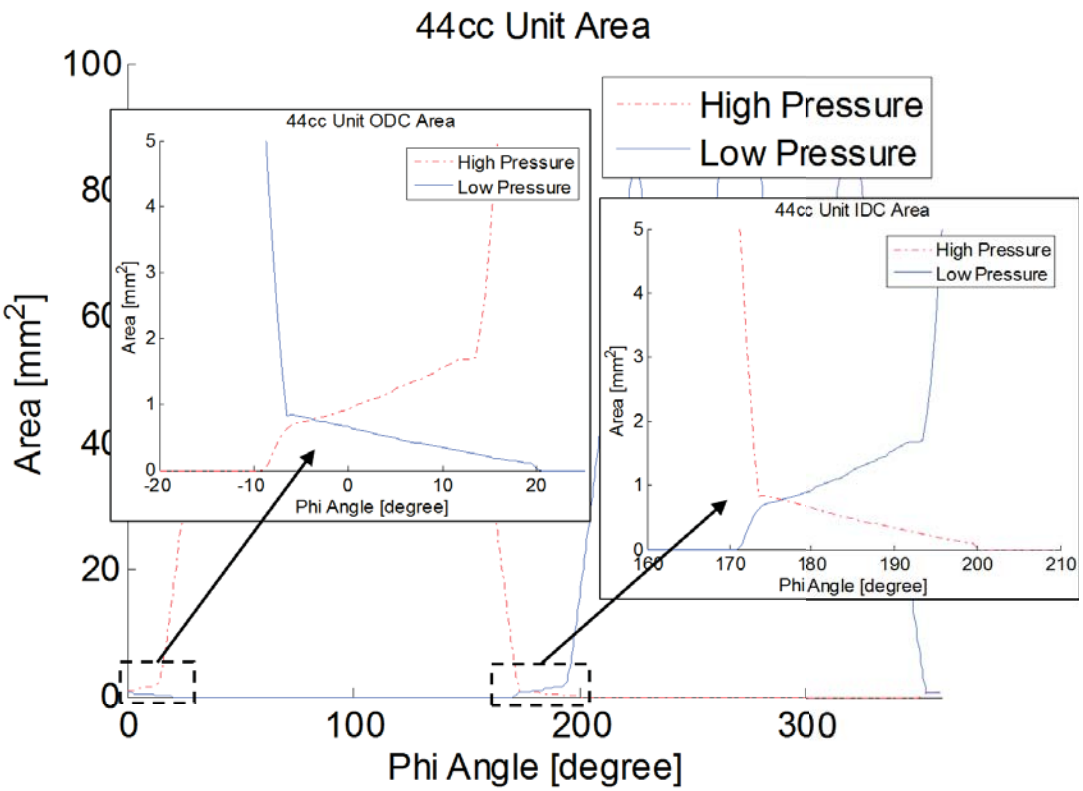

Figure 3.5. Example area file.

Notice there is large portions of the area file where either the high pressure area or the low pressure area is zero. This depicts that the displacement chamber is connected to only one port for the majority of its rotation about the center axis.

A zoomed in image of the areas around ODC and IDC are emphasized due to their enormous influence on the operation of the pump. It is only during expansion and compression of the fluid around ODC and IDC that the orifices flows restricted areas formed by relief grooves play a role in determining the pressure of the displacement chamber.

The area file will become the most crucial inputs to the pressure module, as the design of a particular valve plate can be completely characterized by a given area file (assuming no change in cylinder blocks). Therefore, the rest of this thesis will be centered on the design of the area file.

3.4 Port Pressure

Similar to the displacement chamber, the two ports of the pump are modeled in a lumped parameter approach. The following pressure buildup equation is used to model the pressure of these ports. Notice the main difference is the exclusion of the changing volume, as the ports remain a constant volume. For the sake of notation, I introduce two terms, Q_{rLP} and Q_{rHP} . The discharge flow (Q_{rHP}) can be calculated from the summation of all the individual flows of all displacement chambers to the HP port (Q_{rHPi}).

$$Q_{rHP} = \sum_{i=1}^{z} Q_{rHPi} \tag{3.24}$$

The suction flow (Q_{rLP}) can be calculated from the summation of all the individual flows of all displacement chambers to the LP port (Q_{rLPi}).

$$Q_{rLP} = \sum_{i=1}^{z} Q_{rLPi} \tag{3.25}$$

Where z is the number of pistons (displacement chambers)

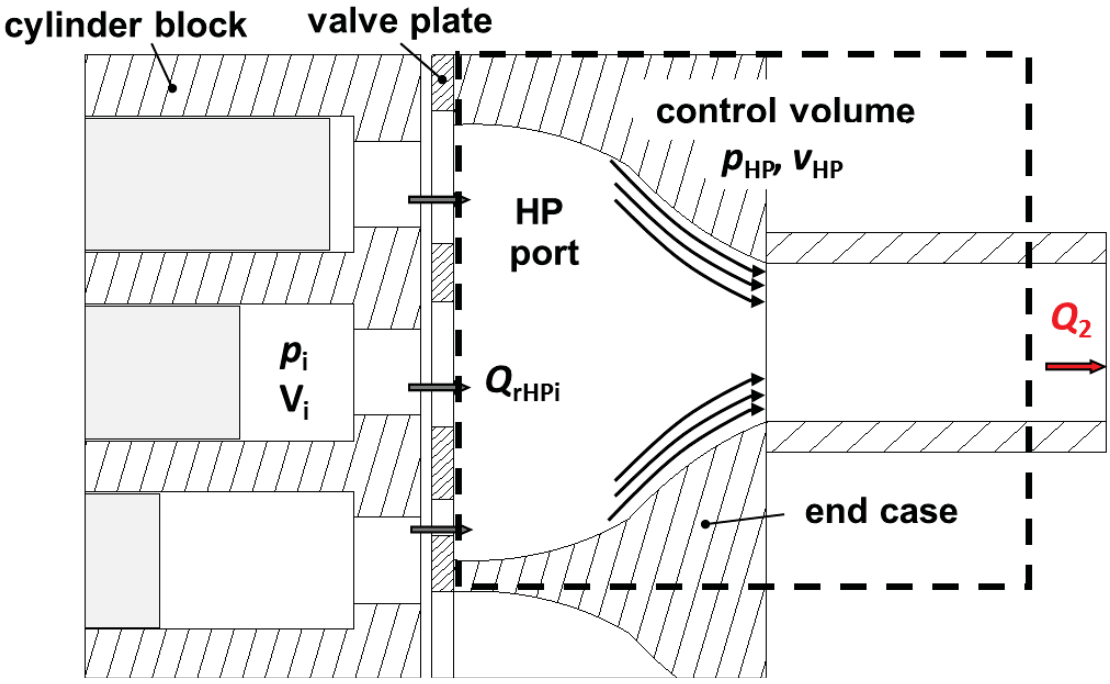

Figure 3.6. Pump port control volume (Klop, 2010).

Using the flows from Eq. (3.24) and Eq. (3.25) we can then derive the pressure in the low and high pressure port,

$$\frac{dp_{LP}}{dt} = \frac{K}{V_{LP}}(Q_1 - Q_{rLP}) \tag{3.26}$$

and

$$\frac{dp_{HP}}{dt} = \frac{K}{V_{HP}}(Q_{rHP} - Q_2)\,, \tag{3.27}$$

where the Q_1 and Q_2 are the entering and exiting flow of the axial piston machine. The direction of the flow depends on the working mode of the axial piston machine. These flows also can be calculated with an orifice equation as we set up in Eq. (3.22),

$$Q_1 = \alpha_{D,LP} \cdot A_{DLP} \cdot \sqrt{\frac{2|p_1 - p_{LP}|}{\rho}}\, sgn(p_1 - p_{LP}) \tag{3.28}$$

and

$$Q_2 = \alpha_{D,HP} \cdot A_{DHP} \cdot \sqrt{\frac{2|p_2 - p_{HP}|}{\rho}}\, sgn(p_2 - p_{HP}) \tag{3.29}$$

Similar to Eq. (3.22) and Eq. (3.23), the areas A_{DHP} and A_{DLP} are important values used to determine the amount of flow entering and exiting the axial piston machine. These areas must be controlled during the calculation to achieve a moderate pressure profile in the displacement chamber. The orifices corresponding to the flows Q_1 and Q_2 are present to model the external load seen by the pump/motor in order to set the correct pressure given the pumps flow rate. The exact values for the areas A_{DHP} and A_{DLP} are therefore dependent also on the other calculated values within the model. This creates interaction loop that must be solved in order for the inlet and outlet pressures to converge to the correct set values. Currently, the implementation with in the model is to control the areas A_{DHP} and A_{DLP} with a PI controller until the pressures P_{LP} and P_{HP} converge to this set values.

3.5 Total System Model

The total fluid model used in order to calculate displacement chamber pressures is depicted in Figure 3.7. Notice each box is a single fluid control volume and all the fluid

with in each control volume is assumed to be at the same pressure, as this model is a lumped parameter model. This model is therefore a system of ordinary differential equations. Each fluid volume's pressure is described using a single differential equation in all the fluid volumes being coupled by the connective orifice flows. The entire system is referred to as the Pressure Module. The essential outputs of the pressure module our the corresponding flow rates and pressures for all the given fluid volumes in orifices for all time steps.

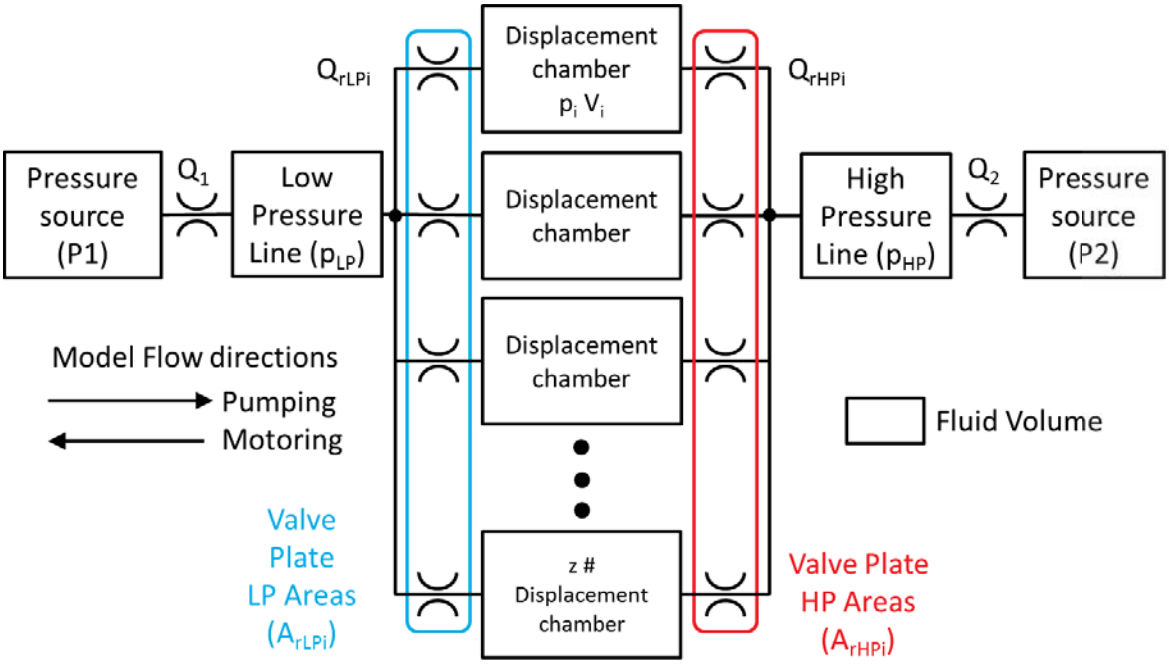

Figure 3.7. Simulation set-up for the modeling of the displacement chamber pressure.

The system of ordinary differential equations is then solved using open source numerical solvers. Traditionally, the solver used within my research group was an explicit Runge-Kutta 5-6 method. An example of a general explicit method is shown in Eq. (3.30).

$$p(t + \Delta t) = p(t) + \frac{dp}{dt}(t) \tag{3.30}$$

This particular system of ordinary differential equations dramatically varies its stiffness. An ordinary differential equation problem is stiff if the solution being sought is varying slowly, but there are nearby solutions that varying rapidly, so the numerical

method must take small steps to obtain satisfactory results. Stiffness in ordinary differential equations is and efficiency issue. Non-stiff solvers can accurately solve stiff differential equations by drastically reducing the time step used. The previous Runge-Kutta solver would vary it simulation times on the order of 15 minutes for low speed operating conditions (stiff) to on the order of 10 seconds for high speed operating conditions (non-stiff). This was due to the fact that the Runge-Kutta solver was not a stiff differential equations solver.

After researching the current stiff solvers available, I found the publication from Heng Li , a research scientist at the Eli and Edythe L. Broad Institute of MIT and Harvard. His research contained a comparative study of various ODE solvers and concluded the LSODA solver was the most efficient. Table 3.1 highlights the conclusions of his study.

Table 3.1. ODE solver comparison (Li, 2009).

Method	#iterations	#evaluations
nr-rkck	1,272	8,772
nr-stifbs*	failed	failed
nr-stiff*	18,272	54,960
lsoda	**381**	**1,754**
gsl-rkck	1,275	11,664
gsl-rkf45	1,315	11,852
gsl-rk2	2,559	13,677
gsl-rk4	961	15,034
gsl-rk8pd	902	16,884
gsl-rk2imp	2,765	56,262
gsl-rk4imp	1,129	33,038
gsl-gear1	>9,999	110,060
gsl-gear2	1,267	36,784
gsl-bsimp*	458	79,914

LSODA is an acronym for Livermore solver for ordinary differential equations: automatic method selection. It is a variant of the solver LSODE (Livermore solver for ordinary differential equations) developed by Linda R. Petzold (Petzold, 1983). LSODA was developed Alan C. Hindmarsh of Lawrence Livermore national laboratories (Hindmarsh, 1983). LSODA solves the same simulations as the Runge-Kutta solver with the simulation time on the order of 3 seconds for all operating conditions. The LSODA solver as compared to the Runge-Kutta solver is on average 100 times faster with the same accuracy. This improvement in the efficiency of the model, as compared to my predecessors, will be crucial in allowing numerous more designs to be simulated.

3.6 Pressure Module Verification

After the pressure module has been simulated for several revolutions in order for the pressures to converge correctly, the pressure module output all the flows and pressures as a function of time involved in the system. The most important pressure is the displacement chamber pressure. This will be later used to calculate most of the performance parameters of the given valve plate design. An example displacement chamber pressure as a function of the rotation angle phi is shown below. Notice the set low pressure is 25 bar and the set high pressure is 350 bar.

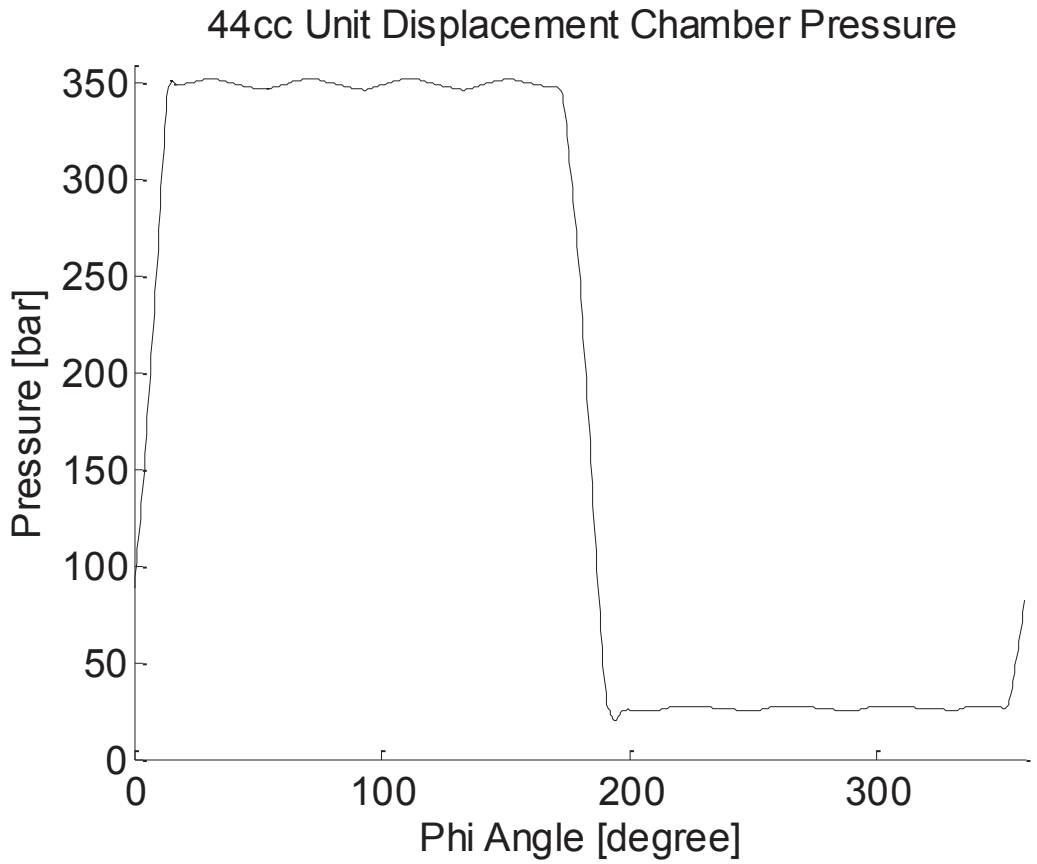

Figure 3.8. Example Displacement Chamber Pressure.

A pump was instrumented with pressure sensor mounted in one of the displacement chambers in the rotating cylinder block. This piezo-electric pressure sensor is able to measure the instantaneous displacement chamber pressure. The signal was wirelessly transmitted to computer to be recorded with a telemetry system. This experimental setup was created in order to a verify the accuracy of the pressure module and as can be seen in Figure 3.9, the pressure module output is very close to measured displacement chamber pressures. This accuracy is what fundamentally enables the success of this computational design methodology.

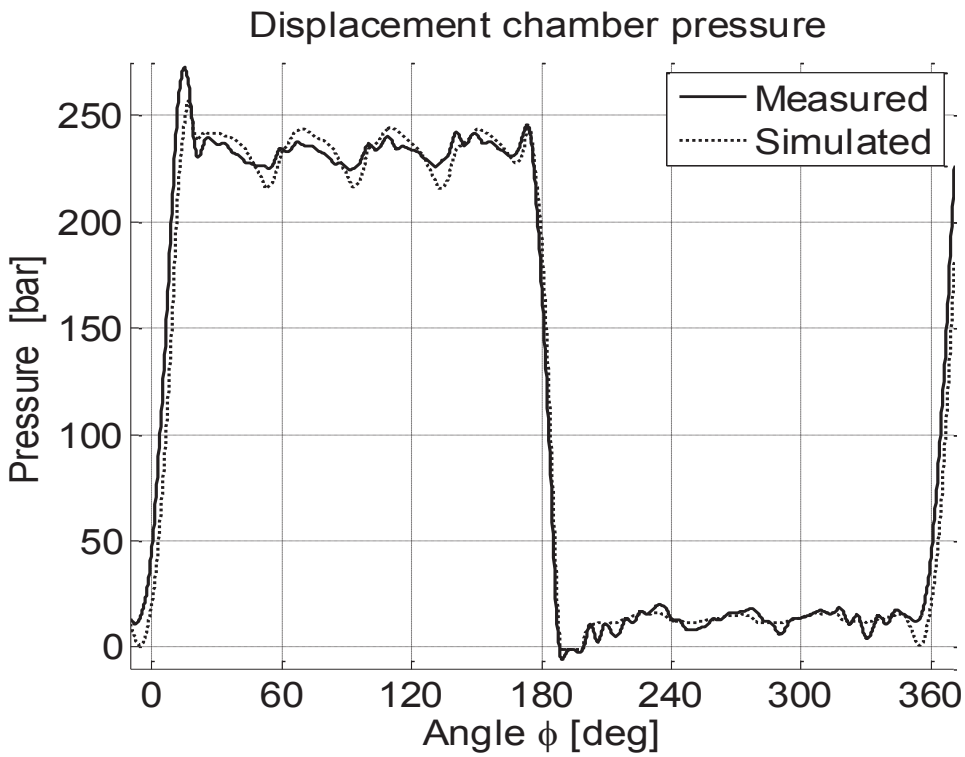

Figure 3.9. Example of pressure module accuracy.

3.7 Important Performance Parameters

After all the pressures and flow rates have been obtained, there are a few important performance parameters that can be calculated to evaluate the quality of the given pump design. These performance parameters will later be used in CHAPTER 4 as objective functions in which to minimize in order to improve the design of the valve plate.

3.7.1 Swash Plate Moments

Oscillating pressures within the pump translate into oscillating forces and moments. The derivation of the swash plate moments follow directly from the previously calculated instantaneous displacement chamber pressures. Upon convergence of the pressure module, all pistons' instantaneous displacement chamber pressures are known. Therefore, given a known surface area of each piston, the instantaneous pressure force (Fp) exerted on the swash plate can be calculated. Notice the net pressure applied to the piston is the difference between the chamber pressures (Fp) in the case pressure (p_1).

$$F_{\mathrm{p}} = A(p - p_{\mathrm{l}}) = \frac{\pi d^2}{4}(p - p_{\mathrm{l}}) \tag{3.31}$$

As the case pressure is relatively constant in the pistons surface area does not change, the force applied on the swash plate by each piston is near linearly proportional to the chamber pressure.

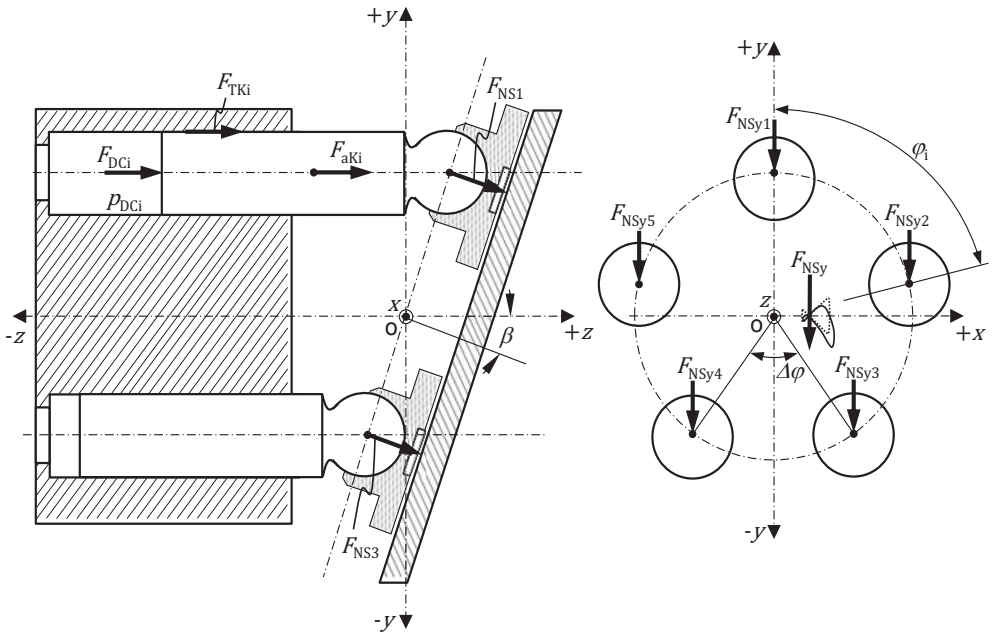

Figure 3.10. Forces acting on the swash plate of a 5 piston pump (Klop, 2010).

For the sake of completion, the pressure force (Fp) is only one of 3 forces applied by each piston to the swash plate. The other 2 forces, specifically the inertia force and the friction force, are small compared to the pressure force and therefore can be neglected while studying the structure borne noise sources. The force and location of every piston is now known in order to calculate the swash plate moments. The swash plate moments M_X, M_Y and M_Z and can be expressed as (Ivantysn & Ivantysynova, 2001):

$$M_{\mathrm{X}} = \frac{R}{\cos^2\beta}\sum_{i=1}^{z} F_{\mathrm{pi}} \cos\varphi_{\mathrm{i}} \tag{3.32}$$

$$M_{\mathrm{Y}} = R\sum_{i=1}^{z} F_{\mathrm{pi}} \sin\varphi_{\mathrm{i}} \tag{3.33}$$

$$M_{\mathrm{Z}} = -R \tan\beta \sum_{i=1}^{z} F_{\mathrm{pi}} \sin\varphi_{\mathrm{i}} \tag{3.34}$$

Eq. (3.32), Eq. (3.33), and Eq. (3.34) calculates each swash plate moment at any given time/rotation angle (φ). An example graph of all 3 directions of swash plate moments for an entire revolution of 44cc (9 piston) pump is shown in Figure 3.11.

These oscillating moments create vibrations of the solid parts of an axial piston machine and are major source of what is referred to in literature as structure borne noise sources (SBNS). These oscillating moments create unwanted periodic vibrations of the swash plate, which get transferred to the exterior case in the surrounding structures. The specific characteristics of the structure will then constitute whether actual acoustic pressure oscillations are created and whether noise is heard. The peak to peak amplitude of each oscillating moment is what quantifies precisely the structure borne noise source.

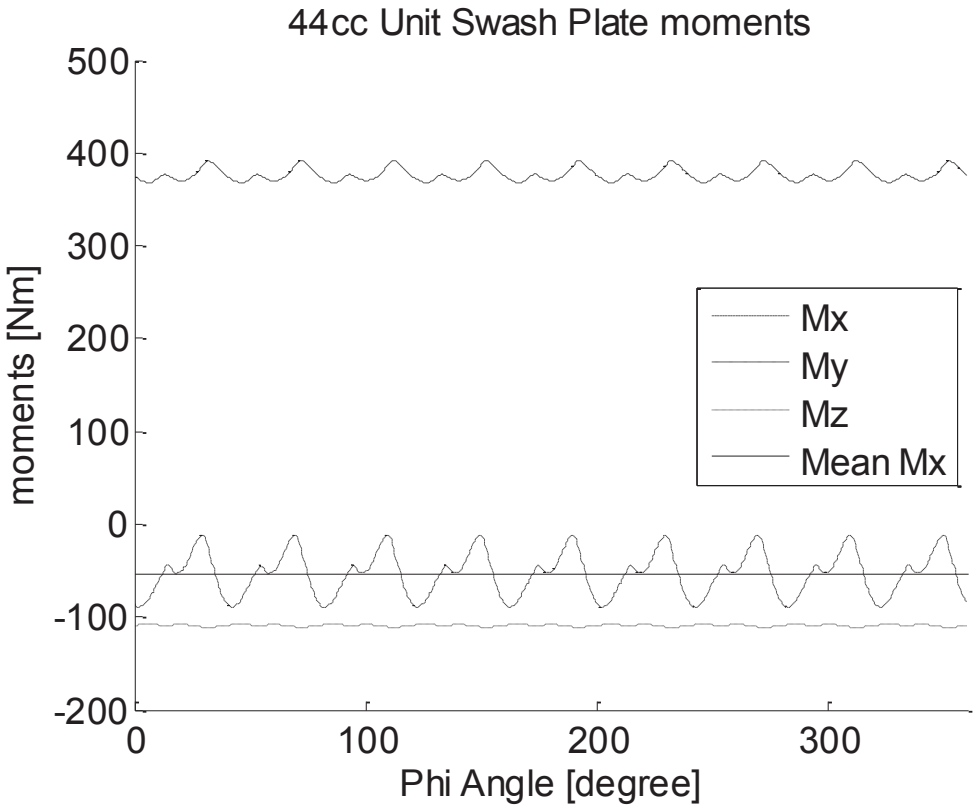

Figure 3.11. Example swash plate moments.

The mean/average of the Mx is also depicted because of its importance. The moment about the X axis (Mx) times a certain lever arm length creates the force that is seen by the pump's control system. Therefore, this mean Mx is proportional to the force that the control cylinder must overcome in order to control the pump's displacement effectively. Increased mean Mx is seen as a disadvantage because at either causes an increase in size of the pump's control system or increased fatigue of the human on pumps that have manually controlled swash plates. Increasing the size of a pump control system has negative consequences, including: increased amount of power to control the displacement, increased losses, greater costs, and slower dynamics.

3.7.2 Discharge Flow Ripple

The instantaneous discharge flow ripple in real displacement units can be accurately simulated through the prediction of several physical phenomena.

3.7.2.1 Kinematic Flow Rate

The instantaneous flow rate being discharged from a pump is not constant. This is due to do discrete number of pistons, each displacing fluid at different times. As can be seen in Figure 3.12, this induces a kinematic flow ripple. The geometric flow rate (Q_{geo}) represents the theoretical mean value of the flow rate.

$$Q_{\mathrm{geo}} = n \cdot z_{\mathrm{K}} \cdot A_{\mathrm{K}} \cdot H_{\mathrm{K}} = n \cdot z_{\mathrm{K}} \cdot \frac{\pi \cdot {d_{\mathrm{K}}}^2}{2} \cdot R_{\mathrm{b}} \cdot tan(\beta) \qquad (3.35)$$

where z_{K} is the number of pistons, n is speed in rev/min, A_{K} is piston area and d_{K} is piston diameter. The instantaneous kinematic flow rate, Q_{kin}, is determined by summing the flows from each i^{th} piston. The theoretical flow rates from each piston are calculated by the product of the piston velocity and area.

$$Q_{\mathrm{kin}} = \sum_{i=1}^{z} Q_{\mathrm{kin,i}} = \sum_{i=1}^{z} v_{\mathrm{ki}} \cdot A_{\mathrm{k}} = \sum_{i=1}^{z} \omega \cdot R_{\mathrm{b}} \cdot tan(\beta) \cdot sin(\varphi_{\mathrm{i}}) \cdot A_{\mathrm{K}} \qquad (3.36)$$

The kinematic flow rate is based solely on the kinematics of the pump and assumes and incompressible fluid. The discharge actual flow rate considers both the kinematic flow

rate as well as the compressibility of the fluid. This flow rate is also extremely sensitive to the design of the valve plate (area file).

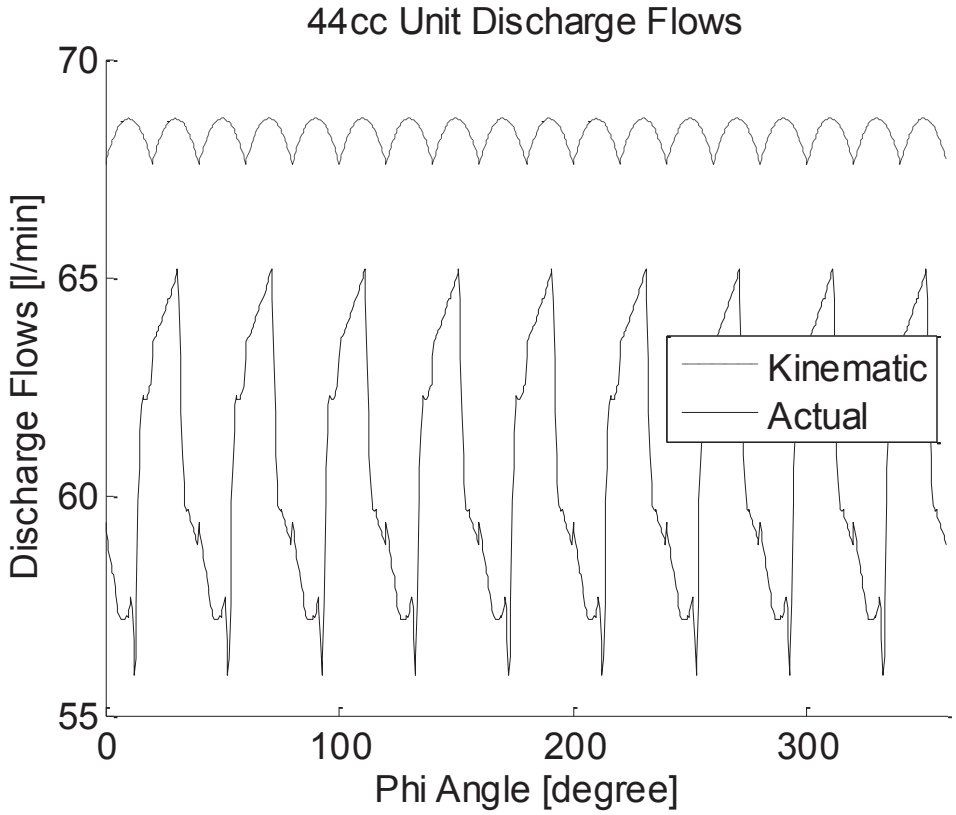

Figure 3.12. Example pump discharge flows.

3.7.2.2 Fluid Compressibility

The compressibility of the fluid describes the decrease in volume with an increase in pressure, given a constant mass. Therefore, as fluid increases in pressure, the volume of that fluid decreases. This decrease in volume must be replaced by either the piston motion or a "back-flow" of fluid from the high pressure port. This work being done on the fluid to compress it is referred to as compression loss because it decreases the amount of fluid displaced by the pump. The valve plate design determines the timing in which this compression work is done. Therefore, controlling the proportion of "back-flow" required to do compression work as compared to piston motion.

3.7.2.3 Cross Porting

There is an additional phenomenon that affects the actual discharge flow of a pump. Near port boundaries (ODC and IDC), the design of a valve plate can allow, for a few degrees, the displacement chamber to be connected to both ports simultaneously. During that time, some high pressure fluid will flow back into the displacement chamber and similarly, some displacement chamber fluid will flow into the low pressure port. This is because the combination of both port flows will enable the pressure in the displacement chamber to be somewhere between the 2 ports enabling fluid flow. This process is called "cross porting" because it allows some fluid to flow from one port through the displacement chamber into the other port. Cross porting will decrease the instantaneous discharge flow rate, and also decrease the total volumetric efficiency of the unit. The advantages of cross porting to affect the other performance parameters, namely: the structure borne noise sources, fluid borne noise sources and control effort outweigh the decreases in volumetric efficiency. However, the priority of this decision is left to the designer and will be explained later in CHAPTER 4.

3.7.2.4 Fluid Borne Noise Sources (SBNS)

The actual discharge flow rate (effective, Q_e), shown in Figure 3.12 includes a combination of the kinematic flow ripple, compression of the fluid, and the cross porting due to the design of the valve plate. The combination of cross porting, and fluid compressibility greatly increases the peak to peak (maximum – minimum) amplitude of the discharge flow. This amplitude (ΔQ_{hp}) is referred to in literature as the fluid borne noise source (FBNS). This flow ripple generated by the pump transmit throughout the entire hydraulic system inducing vibrations of other components, potentially causing airborne noise (ABN) heard by human ears. These flow ripples can also cause complications in the control of hydraulic systems. In flow ripple combined with a load creates pressure ripples. These pressure ripples create proportional force ripples which can cause violent oscillations in the physical structure of the machine. Reducing the flow ripples caused by a pump creates quieter and safer hydraulic systems.

3.7.3 Volumetric Efficiency*

The effective discharge flow rate of a real pump (Q_e) is determined from the difference between the derived (theoretical) output flow (Q_{geo}) and the sum of all the volumetric losses (Q_s) (Ivantysn & Ivantysynova, 2001).

$$Q_{\mathrm{e}} = Q_{\mathrm{geo}} - Q_{\mathrm{S}} \tag{3.37}$$

The volumetric losses (Q_s) are the total sum of all the internal and external volumetric flow losses (Qs).

$$Q_{\mathrm{S}} = Q_{\mathrm{Se}} + Q_{\mathrm{Si}} + Q_{\mathrm{Sf}} + Q_{\mathrm{Sk}} \tag{3.38}$$

Where Q_{se} is the total volumetric flow occurring from the displacement chamber through the lubricating interfaces. In literature, these flows are referred to as external volumetric losses or external leakages (Figure 3.3).

$$Q_{\mathrm{Se}} = Q_{\mathrm{SK}} + Q_{\mathrm{SG}} + Q_{\mathrm{SB}} \tag{3.39}$$

The total gap flow QSI, flowing back to the inlet, belong to the internal volumetric losses. QSf, according to ISO 4391, are losses due to incomplete filling of the displacement chamber. Finally, Q_{Sk} are the volumetric losses due to the compressibility of the fluid. The volumetric efficiency (η_v) then follows as the ratio of the effective discharge flow rate in the theoretical discharge flow rate.

$$\eta_v = \frac{Q_{\mathrm{e}}}{Q_{\mathrm{geo}}} \tag{3.40}$$

The valve plate influence on the external leakage flows (Q_{Se}) is negligible. Modeling the external leakage flows has been shown to be an extremely complicated process. Therefore, the external leakage flows can be neglected in the pump model. To distinguish from the true volumetric losses (Q_s), I introduce the term leakage(s)*to refer only to the internal leakages (due to back flow and cross porting) and compression losses.

$$Q_{\mathrm{S}}{}^{*} = (Q_{\mathrm{Si}} + Q_{\mathrm{Sk}}) \tag{3.41}$$

Similarly, to distinguish from true volumetric efficiency, a term is defined as volumetric efficiency* (η_v*).

$$\eta_v{}^{*} = \frac{Q_{\mathrm{e}}{}^{*}}{Q_{\mathrm{geo}}} \tag{3.42}$$

Where (Qe*) only includes (Q_s*).

$$Q_e{}^* = Q_{geo} - Q_S{}^* \tag{3.43}$$

Figure 3.13 shows the instantaneous volumetric efficiency* for one revolution of a 44cc pump (example valve plate). The oscillations in the discharge flow ripple can be seen also in the volumetric efficiency therefore, the average over one revolution is used later in CHAPTER 4. Sometimes leakage* will be displayed in percent of theoretical flow rate.

$$Q_S{}^*[\%] = \frac{Q_S{}^*}{Q_{geo}} \cdot 100 \tag{3.44}$$

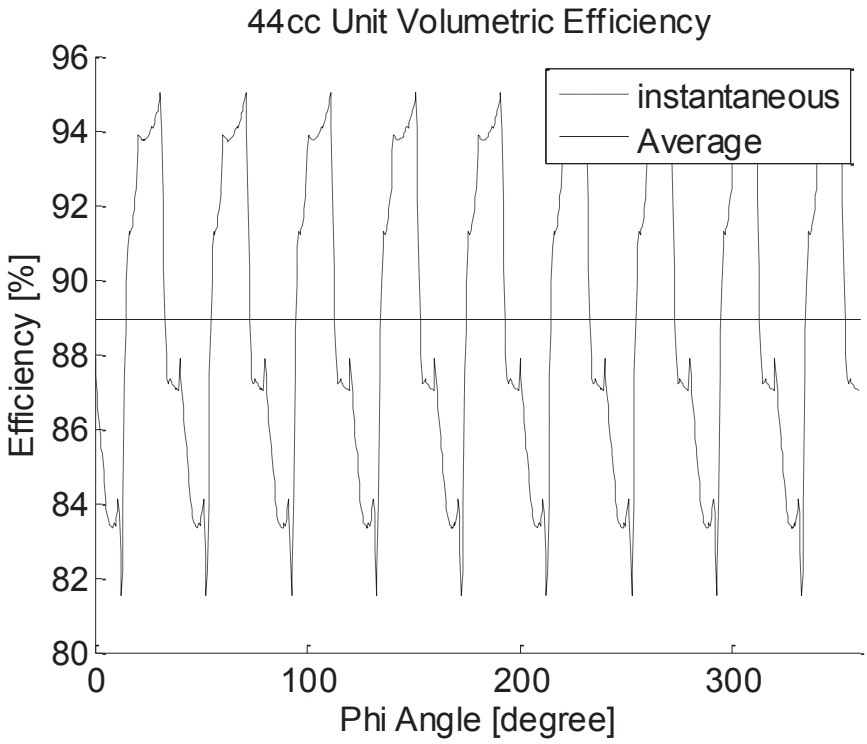

Figure 3.13. Example Volumetric efficiency*.

3.7.4 Cavitation

Cavitation refers to the localized formation and subsequent collapse of gas bubbles within a fluid. Gas (usually air) is absorbed into a fluid until the concentrations of gas reach saturation point. The saturation point of the gas depends on multiple factors including the oil, temperature, and pressure. Absorbed gas in a fluid does not affect the physical properties of the fluid until the gas comes out of solution. This release of gas

bubbles into the fluid usually occurs in specific parts of a system that cause the fluids temperature or pressure to change past a safe point. This usually occurs in the suction port of a pump which is designed improperly allows the pressure to become too low. Undissolved bubbles will subsequently collapse once the pressure rises faster than the absorption rate. Cavitation is dangerous because it drastically decreases the fluid bulk modulus, extreme high noise levels, and extreme shockwaves from the collapse of the bubbles. The shockwaves cause erosion on the surfaces of the pump. This erosion pits the components of the hydraulic system weakening the structures and introducing contamination into the fluid.

Although cavitation is very dangerous, complex and unpredictable, it can be easily avoided to the proper design of the hydraulic system. Cavitation can be avoided in a system through proper reservoir sizing, hydraulic line sizing, and anti-cavitation check valves. Cavitation can be avoided inside the displacement chamber of a pump through the design of the valve plate by not allowing the pressure in the displacement chamber or ports to drop below a specified amount.

3.8 Parallel Architecture

The advancements in computer architectures have led computer manufacturers to develop the idea of multi-core processors (CPUs). The transition from singles core processors to multicore processors was motivated by the relationship between the power dissipation of a CPU and its clock frequency. Before multicore processors CPU manufacturers would consistently increase the clocking frequency of the CPU in order to improve performance. This design methodology saturated at certain power consumption due to issues with heat. The computer manufacturers could no longer cool the processors fast enough to account for the increase in power dissipation and decrease in size (surface area). This advancement has enabled computer manufacturers to continue to abide by "Moore's Law", that predicted a doubling of transistors on a CPU every 2 years.

The major disadvantage to this fundamental change in CPU architecture is seen by the software developers for the programs running on these architectures. A software developer must now design every program to utilize the advancements in multicore

processors in order to utilize the improvements in competition speeds. This, however, cannot be accomplished for every program, depending on its concurrency. Concurrency, in computer science, is a property of systems in which several computations are executing simultaneously and potentially interacting with each other. The software developer must understand the logic implemented within the software in order to identify the amount of concurrency in every program. Only programs that have concurrency can benefit from dividing up the simultaneous executions onto various cores (threads) within the processor. Similarly, old software written before multicore processors must be rewritten to be converted from sequential implementations to parallel implementations.

3.8.1 Single Machine Implementation

Seeniraj (2009) developed his valve plate design software into a single sequential implementation of an executable termed “VpOptim.exe”. Furthermore, his preprocessing, and post processing portions of his valve plate design algorithm were written in Matlab **(**Figure 2.2. Seeniraj algorithm). In order to utilize the advancements in multicore processors, VpOptim.exe was studied to maximize the concurrency within the program. The software was then retrofitted using the compiler library OpenMP in order to create a parallelized (shared memory) implementation of VpOptim.

VpOptim was found to have a considerable amount of concurrency. Within the main function of the program, there were 2 loops (nested for loops) in order to perform a full factorial search for every combination of valve plate (VP) and operating condition (Opcon). These 2 loops were converted into a single loop and that single loop was parallelized to perform different iterations of the loop on the various threads (CPU cores).

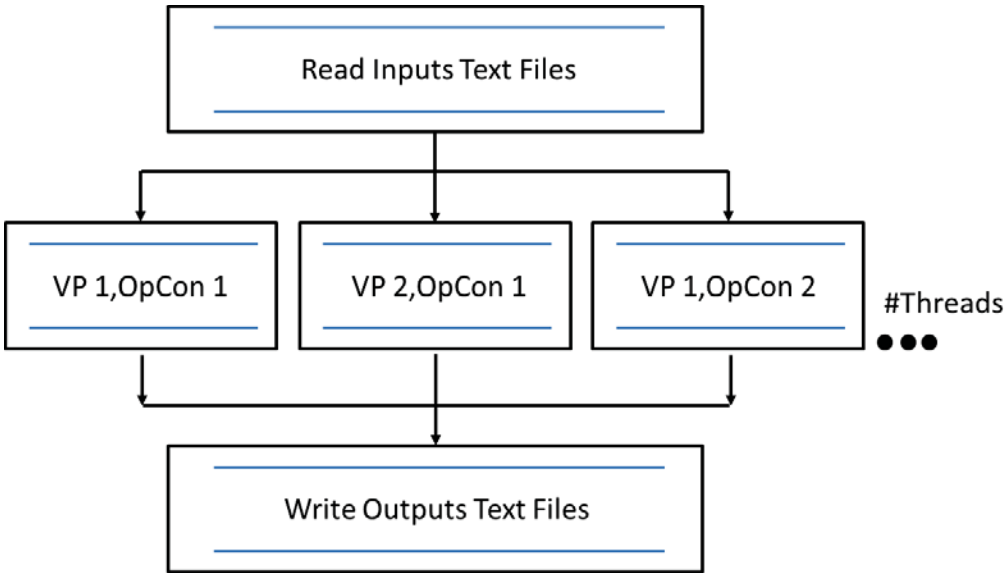

Figure 3.14. VpOptim Program Structure.

A speed improvement study was performed in order to verify the success of the parallel implementation and also to tune the number of threads in order to maximize the greatest speed improvement as compared to the sequential version (1 thread).

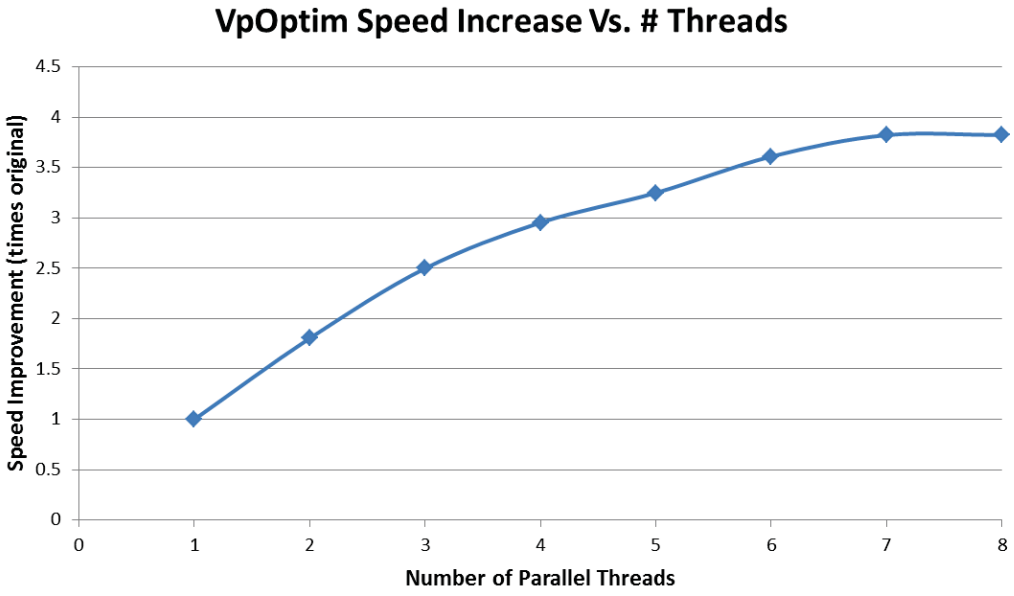

Figure 3.15. VpOptim speed improvements.

VpOptim's results were compared with the classic Amdahl's Law and order to estimate the amount of concurrency (empirical) found within VpOptim. As can be seen in Figure 3.16. Amdahl's law, the estimated parallel portion was around 85%.

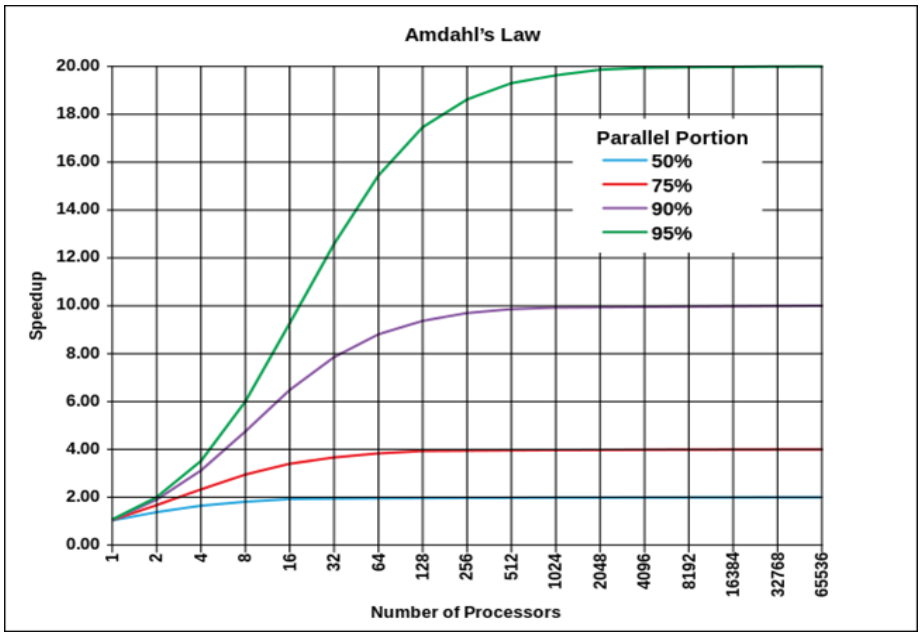

Figure 3.16. Amdahl's law.

3.8.2 Multiple Machine Implementation

An additional framework was developed outside the VpOptim.exe in order to parallelize the computations of valve plate designs on a cluster of computers (variable amount). The distributed memory implementation was developed independent of the now parallelized VpOptim.exe to include potential users of VpOptim without the access to computer clusters and also provide the scalability support for clients that do have access to multiple computers.

The distributed memory implementation was created using Windows Communication Foundation (WCF). This framework consists of 3 main parts: The server, submitter, and worker. After the initial set up in communications have been established by the various components, a typical work cycle begins with the submitter. Given a list of valve plates by the user, the submitter reads in the valve plates and sends the list to the server. The server is the controlling element and divides the given list of valve plates into

segments. The segments of valve plates are then passed to each worker to be evaluated. The workers run continuously on the various computers used for simulations. Their job is to accept the given valve plate inputs, execute VpOptim.exe, and return the outputs to the server. When all the output files have been returned to the server, the server will pass the output files back to the submitter and the submitter will write the output text file in its current directory.

This two-tier framework using Windows Communication Foundation (WCF) and the OpenMP compiler for VpOptim.exe has shown to be very scalable and robust. The relatively low overhead needed to distribute the memory on multiple machines has allowed the computation time of valve plates to be nearly linearly inversely proportional to the number of machines.

3.9 Valve Plate Design Space

As explained in Section 3.3, the geometry of the valve plate is described in the area file. Most important sections of the area file/valve plate are at the port boundaries. The two port boundaries are labeled ODC (outer dead center) and IDC (inner dead center).

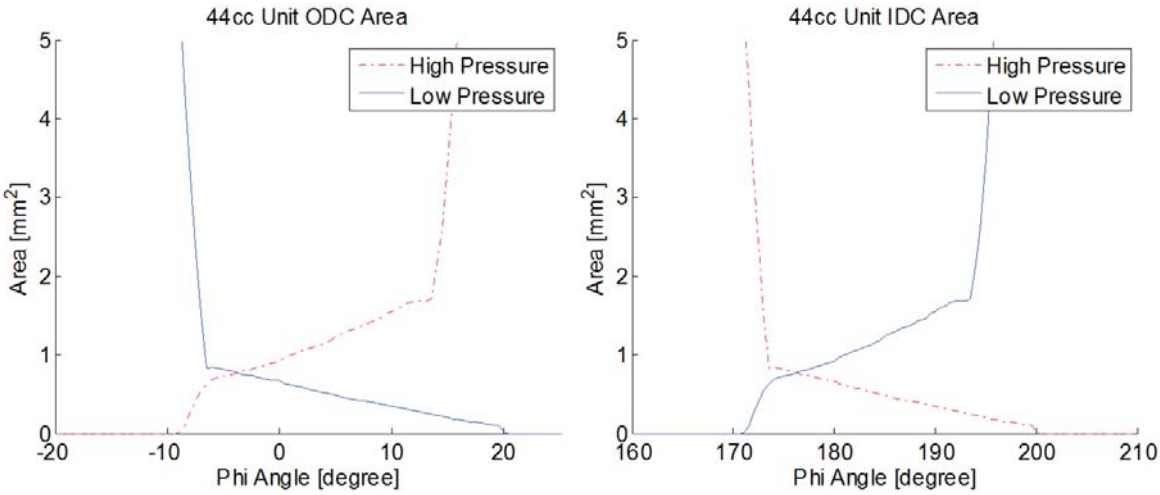

Figure 3.17. Example ODC and IDC Areas.

Each boundary has decreasing opening areas to one port, while simultaneously increasing the opening areas to the other port. As discussed in Section 2.1, relief grooves

design was introduced in order to control these boundaries with greater fidelity. It is therefore sufficient to characterize the entire valve plate geometry (area file) with the description of these important areas of flow restriction located in the regions close to ODC and IDC.

3.9.1 Valve Plate Groove Numbering

To organize the multiple relief grooves, a convention was set in order to precisely map the modeled area files to real valve plate geometries. Figure 3.18 shows the groove numberings relative to the conventional coordinate system defined at the Maha fluid power research center when the displacement unit is operating in pumping mode.

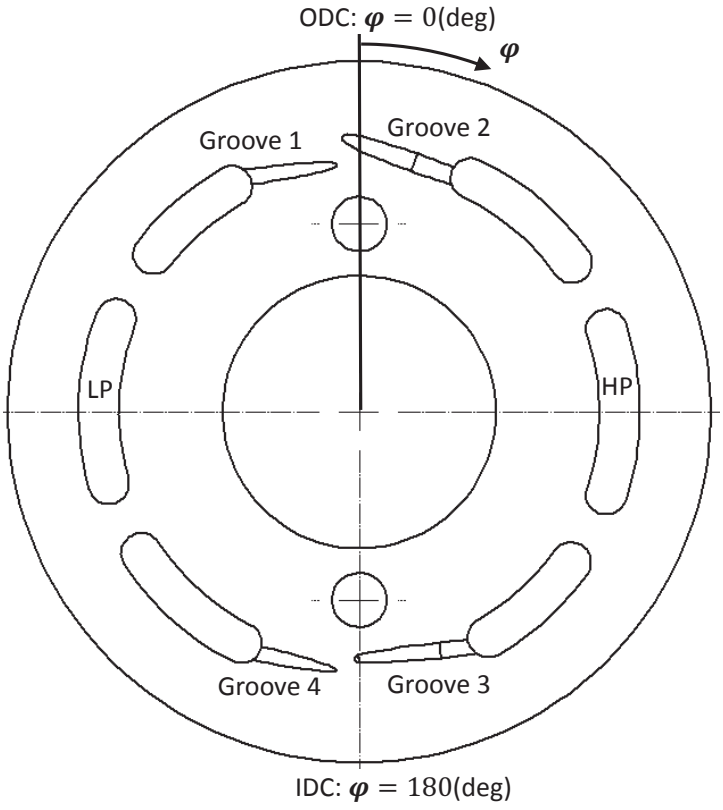

Figure 3.18. Valve plate groove numbers.

This numbering system has been changed since Seeniraj (2009) and Kim (2012) because it is more intuitive to the physics of the valve plate design problem. When a displacement chamber is near ODC is simultaneously influenced by both grooves 1 and 2.

Therefore, it is natural to number these grooves adjacently and likewise grooves 3 and 4. This aids the user of VpOptim to more efficiently process and understand the input files. The post processing of nearly 20,000,000 valve plate designs has motivated the removal of unnecessary complications that cause confusion and mistakes within this research study.

More importantly, a subtlety in the physics motivates numbering Groove 1 first, even though it has the highest values for φ. Assuming the rotation of the displacement chamber is clockwise (CW), used in the convention, the displacement chamber is affected by Groove 1 before Groove2. It is important for the designer to understand this relationship, so the numbering system was changed in order to aid in understanding.

3.9.2 Parameterization of Groove Area

It is very common in engineering and design to organize designs through the use of a set of numbers. This process known as parameterization is a mathematical process of deciding and defining the parameters necessary to describe a complete specification of a model. Simple parameterizations include the representation of an entire line using the well-known slope and y-axis intercept formula other line. The parameterization of a model (grooves) also controls the degrees of freedom in which the possible designs can realize.

The parameterization of a model is not unique and the same geometric object can be described using multiple parameterization schemes. For example, a line can be described using the point slope (3 variables) and also the coordinates of two points (4 variables). This example highlights an important fact that not all parametrizations are equal and that some are simpler (having less variables) than others. It will be shown later that the complexity of the design of experiments increases exponentially with the number of variables. It is therefore very important to reduce the number of variables in the parameterization of the relief grooves.

3.9.2.1 Nonlinear Groove Shape

The traditional relief groove geometry has a corresponding area as shown in Figure 3.23. Groove area for linear relief grooveI labeled these grooves linear grooves for

obvious reasons. The choice of linearly shaped relief groves is assumed to chosen for simplicity because there is no explanation in literature.

The switch from linear to nonlinear grooves came about for three reasons. Firstly, then valve plates cannot physically be manufactured with linear grooves. A linear groove would cause a very sharp angle cut in the metal. Because of concentrated stresses on sharp discontinuities the valve plate which shear and crack during normal operations. Therefore, thin valve plates must have a round hole drilled at the beginning of the grooves to distribute the stresses.

Secondly, during previous research with linear grooves, it was found that grooves with an "offset" have better ΔMx performance. The offset was a crude nonrealistic step by simply shifting all of the groove areas up by the same amount. While this gave good results, these designs were not manufacturable.

Lastly, the circular nature of the nonlinear groove came from the common practice of manufacturing valve plates by cutting the surface of the plates using ball end mills. The nonlinear groove was then created to allow in initial offset to increase the ΔMx performance with only small changes to the current manufacturing processes of valve plates. The ellipse shape was implemented instead of a circular shape due to the simple fact that the units of an area file are arbitrary and there is no physical reason restrict area files to mm^2 per degree. Also, the linear portion is always set to be tangential to the ellipse to create a realistic continuity of a ball end mill making a cut through the material.

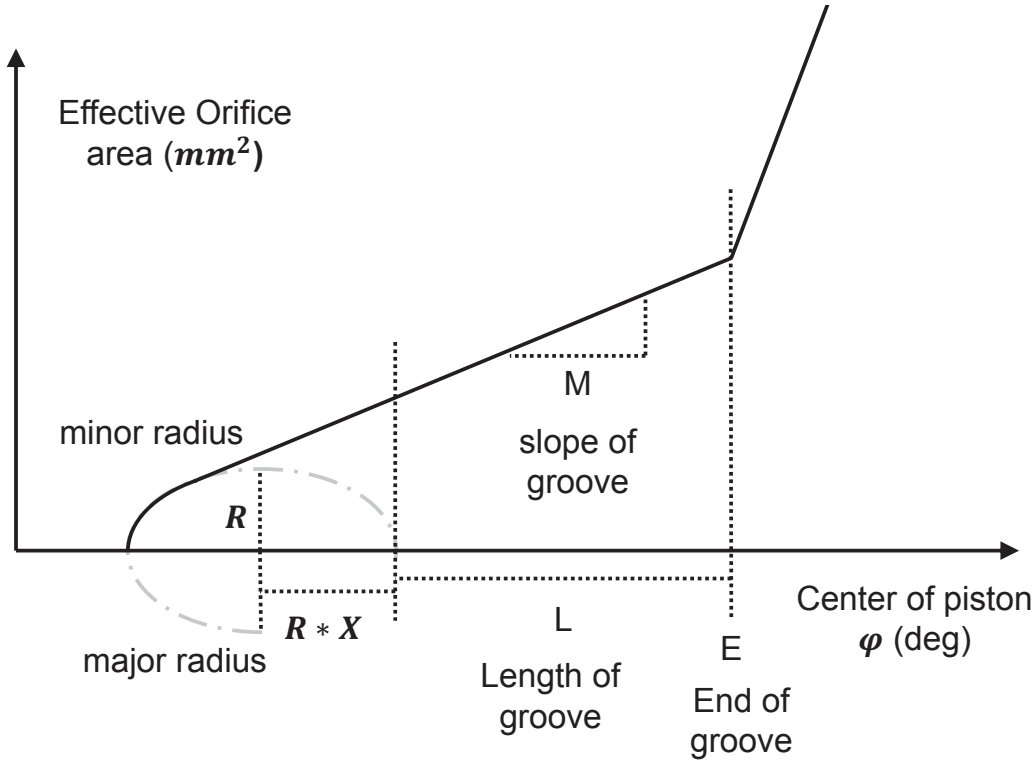

Figure 3.19. Nonlinear Groove Area.

3.9.2.2 Variable Selection

As mentioned previously, the same basic shape (geometric object) can be described using multiple sets of variables. The specific set of variables chosen to parameterize the nonlinear groove shape, were chosen for three main reasons.

Firstly, the specific variables chosen were very important in order to aid the optimization algorithm in making correlations between inputs and outputs. If all of the good designs require a complicated combination of all the input variables it makes it more difficult for search algorithm to stumble upon these. These decisions were based on observations seen within previous case studies. The most important observation being the "end of the groove, E" is the least sensitive variable to all the performance parameters. This makes it a very likely candidate to have other variables be dependent on the eve value and still maximize simplicity. The second variable chosen for this fact is the "slope of the groove, M". An alternate to the slope of the groove would have been the height

(area) at the end of the groove (at E). M was chosen based on experience (also seen in literature) that the rate of pressure rise correlates well with performance parameters.

The second reason to choose certain variables was the idea of variable orthogonality, or variable independence. The variables are given set of lower bounds and upper bounds for each variable independently. It is therefore more efficient to parameterize the grooves to maximize the amount of realistic designs found within the combination of all the variable boundaries.

Table 3.2. Groove variable boundaries.

Variable	**Lower Bound**	**Upper Bound**	**Units**
e1	-15	-5	[deg]
e2	5	15	[deg]
e3	-15	-5	[deg]
e4	5	15	[deg]
l1	0	30	[deg]
l2	0	30	[deg]
l3	0	30	[deg]
l4	0	30	[deg]
r1	0	2	[mm^2]
r2	0	2	[mm^2]
r3	0	2	[mm^2]
r4	0	2	[mm^2]
x1	1	15	[unit less]
x2	1	15	[unit less]
x3	1	15	[unit less]

Table 3.2. Continued.

x4	1	15	[unit less]
m1	0.01	0.1	[mm^2/deg]
m2	0.01	0.1	[mm^2/deg]
m3	0.01	0.1	[mm^2/deg]
m4	0.01	0.1	[mm^2/deg]

The use of the variable L (length of groove) was chosen because it can be selected independent from the other variables. An alternative to L, would have been S (the start of the groove). S would have been dependent on the E and vice versa. S must come before E. It becomes difficult to implement logic to safeguard all the possible combinations of S coming after E. The use of the variable L solves this problem in a very simple and robust manner. L also correlates very well to the volumetric efficiency because it determines the amount of cross porting.

The variable X, (radius multiplier) was also chosen so that X can be independent of all R. All successful valve plates had the major axis of the ellipse along the horizontal axis (Figure 3.19). By choosing a multiplier of only positive values, this restricts the horizontal radius to always be larger and also be independent of the chosen vertical axis, R.

Thirdly, the current set of parameterization variables allows the designer to easily limit the possible designs to older reduction techniques, such as ideal timing and linear relief grooves. This would only be done due to limits in manufacturing, cost, or comparative studies. This is later explained in Section 3.9.3. “Backwards Compatibility”

3.9.2.3 Groove Symmetry

Historically, it was common to assume certain symmetry of the valve plate (grooves) in order to simplify the design process. Motor valve plates are usually designed in a symmetric way because of the operation in both direction of rotation. Likewise units which run in pumping and motoring might profit from symmetrical designs. Referring to

Figure 3.18, the valve plates are labeled to have the same groove area for grooves 2 and 4 (4 = 2) and independently groove 3 and 1 (3 = 1). Previous design studies have revealed a problem that could not be solved using the traditional symmetric groove constraint. The constraints of symmetric grooves forced me to choose between pressure peaks at ODC or IDC. This was the motivation to decouple the ODC and IDC grooves thus creating asymmetric grooves. Asymmetric grooves are simply all 4 grooves designed independently. To the best of my knowledge, this is the first time that asymmetric grooves were introduced. The only negative consequence of using asymmetric grooves is the increased design space complexity and increase in computational time required. The improvements to the modeling in other areas (solver, optimization algorithm) which were proposed within this research study more than compensate for this consequence.

The asymmetric grooves are automatically backwards compatible and if the symmetric groove is the best design for balancing pumping mode and motoring mode, the algorithm will automatically find such designs.

3.9.3 Backwards Compatibility

In the interest of allowing the greatest possible combinations of designs and reduction methods, nonlinear groove areas can be easily constrained to study old reduction methods. These reduction methods can also naturally result from the optimization algorithm if they happen to give the best results (performance parameters).

3.9.3.1 Ideal Timing

Ideal timing was the first reduction technique and is obtained by cutting the openings in the valve plate to a specific location. This is the most simple design technique for valve plates, but it is still used in industry because of its low cost manufacturing process.

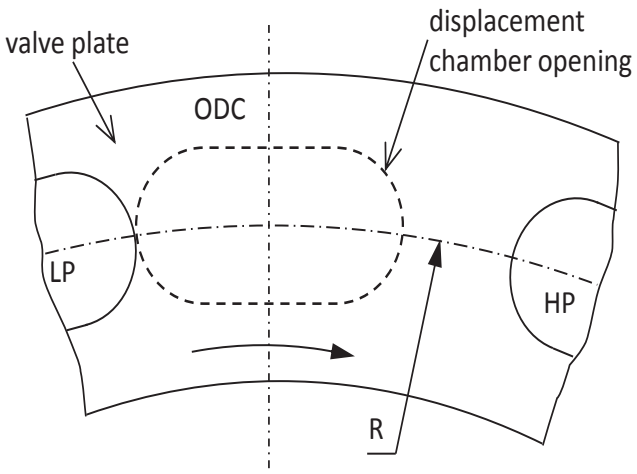

Figure 3.20. Valve plate with ideal timing.

To constrain the current nonlinear grooves to only ideal timing, the designer simply sets the lower bound and upper bound of all the L (length of groove) variables to 0. This will create an area file similar to that of Figure 3.21.

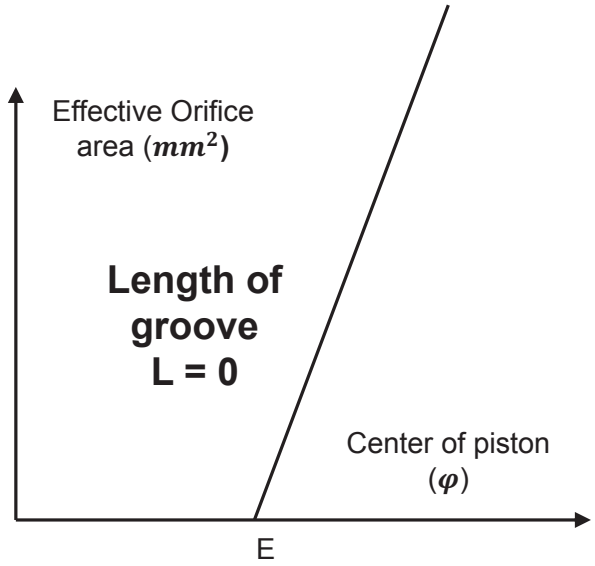

Figure 3.21. Groove Area for ideal timing.

3.9.3.2 Linear Relief Grooves

Linear grooves were introduced in the state-of-the-art chapter in the traditional relief grooves found in literature. Linear grooves are the predominant style of relief grooves found currently in practice. This is mainly due to the limitations of the design

process. Linear grooves are still useful because they give the best flow ripple $\Delta Q_{hp.}$ They will naturally result from the optimization algorithms for designs with high priority on flow ripple.

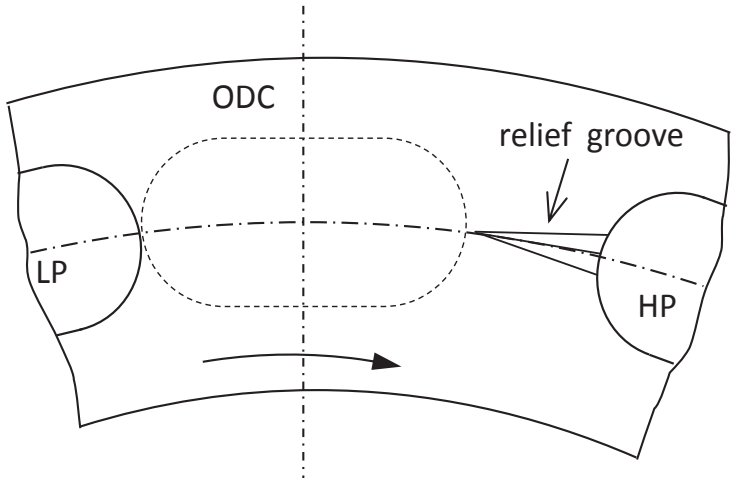

Figure 3.22. Valve plate with linear relief groove.

Linear (or near linear) grooves can be identified by grooves that have small values of R. to purposely constrain the nonlinear grooves back to linear grooves, the designer only needs to set the lower bound and upper bound of the 4 R values to 0.

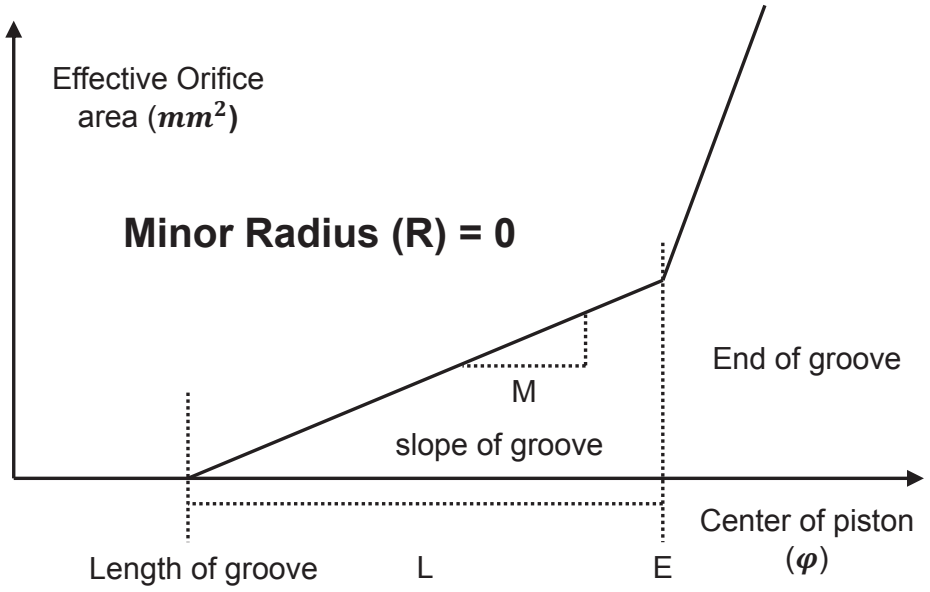

Figure 3.23. Groove area for linear relief groove.

3.9.3.3 Indexing

Indexing is another common reduction techniques found in industry. Historically, indexing was a simple and cheap way of testing different valve plate designs without the need of manufacturing new valve plates. First, a reference valve plate was designed (symmetric). Second, that valve plate was rotated and reinstalled with an index value (rotation angles in degrees) relative to the first reference valve plate. It is important to understand that indexing always is relative to another valve plate.

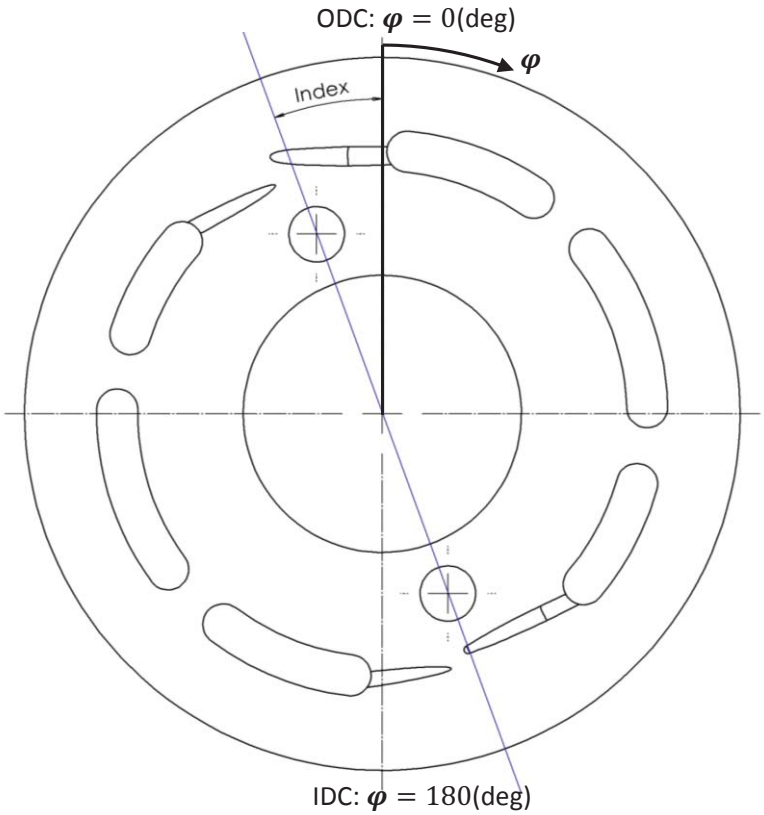

Figure 3.24. Valve plate indexing.

Asymmetric relief grooves automatically incorporate all of the various indexing values. Asymmetric relief grooves, not only incorporate indexing, but essentially allows the possible indexing of every groove independently, and is much more comprehensive. However, although it is not recommended, a designer can simulate indexing by simply changing the E (end of groove) by the same amount for every groove. This will artificially rotate the reference design similar to indexing.

3.10 Additional Pressure Module Features

There is a reduction technique known as filter volumes. A filter volume that influences the displacement chamber pressure near ODC is referred to as a pre-compression filter volume (PCFV). A filter volume that influences the displacement chamber near IDC is referred to as a decompression filter volume (DCFV). Every axial piston machine has a valve plate, but only a subset of pump manufacturers incorporate filter volumes into the design of the pump. The filter volume communicates with the displacement chamber through the valve plate. Therefore for these pumps, it is part of the valve plate design, but filter volumes also require additional changes to the pump and is therefore categorize as a specialty function within this thesis. The filter volumes are parameterized similar to the grooves and the variables are shown in Table 3.3.

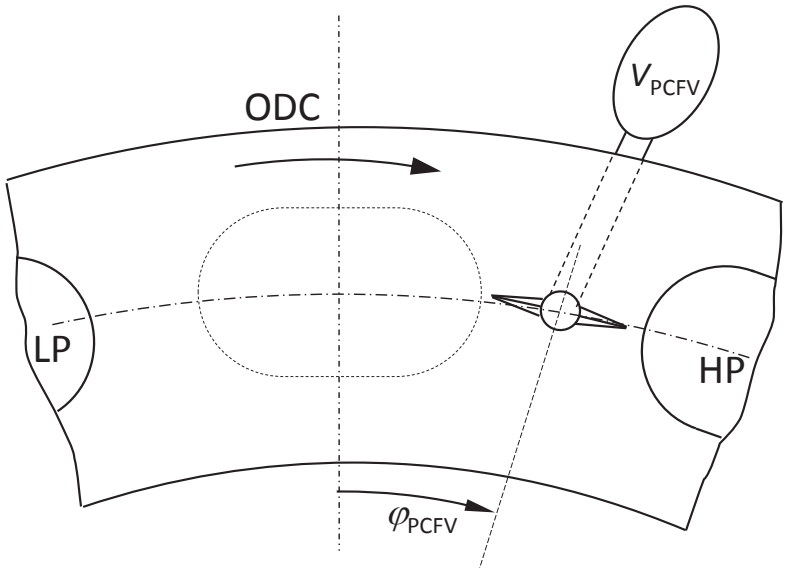

Figure 3.25. Valve plate with pre-compression filter volume.

Table 3.3. Filter volume variable boundaries.

Variable	Lower Bound	Upper Bound	Units

ϕ_{SPCFV}	0.22	0.22	[deg]
ϕ_{PCFV}	2	2	[deg]
m_{PCFV}	4	4	[mm^2/deg]
ϕ_{SDCFV}	0.22	0.22	[deg]
ϕ_{DCFV}	182	182	[deg]
m_{PCFV}	184	184	[mm^2/deg]
r_{PCFV}	0.0012	0.0012	[deg]
V_{PCFV}	9e-5	9e-5	[deg]

One final design technique that is included within the valve plate design is an air release port. This technique is characterized by allowing the displacement chamber to be connected to the case fluid in order to influence the chamber pressure. Similar to a filter volume, the air release port(s) are cut into the valve plate. Air release ports can be simulated for an existing design for comparison purposes, but are not used to design future valve plates because relief grooves can solve all of the same problems as an air release port without as many of the negative consequences.

CHAPTER 4. DESIGN METHODOLOGY

4.1 Optimization Problem Statement

The design of a valve plate can be a subjective task. First, the precise problem in which to be solved must be clearly defined. Secondly, the methodologies for solving such a problem can then be explained. In general, and mathematical optimization problem consists of minimizing an objective function, f, which is a function of a set of design variables $\overline{\boldsymbol{x}}$.

$$minimize\ f(\overline{\boldsymbol{x}}) = [X_1, X_2, X_3, X_4, \dots, X_n] \tag{4.1}$$

Most real-world applications require additional constraints to be placed upon the design variables. These constraint functions are also functions of the design variables. These are characterized by two main groups, the set of inequality constraints.

$$g_1(\overline{\boldsymbol{x}}) \leq Limit \tag{4.2}$$

And equality constraints

$$h_1(\overline{\boldsymbol{x}}) = Limit \tag{4.3}$$

The classifications of these constraints are motivated by the differences in which many classical optimization algorithms handle these two classes of constraint separately.

4.1.1 Design Variables

Section 3.9. discusses the parameterization of the area files. Each group is defined by five variables and therefore every design using asymmetric nonlinear grooves has 20 design variables for the valve plate and an additional 8 for the filter volumes. The input vector $(\overline{\boldsymbol{x}})$ is 28 variables long.

$$\bar{x} = [X_1, X_2, X_3, X_4, \dots, X_n] \quad (4.4)$$

The optimization problem is stated as only functions of the design variables. There are additional variables needed to simulate the pressure module, but they are not design variables and therefore are constant and not considered as part of the optimization problem statement. In the future, a designer can choose to convert any variable to a design variable, therefore increasing $\bar{x}$. Table 3.2 outlines the 20 design variables used in the design of a valve plate.

4.1.2 Objective Functions

The design of a valve plate is one example of the class of optimization problems known as Multiobjective Optimization. Multiobjective optimization is the field of minimizing multiple objective functions simultaneously. The objective functions are based on the previously discussed performance parameters. The performance parameters have been defined in such a way to easily translate into objective functions. There are five performance parameters used for objective functions currently. All five of these performance parameters are defined such that minimizing these functions increase the performance of the pump.

Minimize: For All Operating Conditions

$f_1(\bar{x})$ = Leakage* [%]

$f_2(\bar{x}) = \Delta Q_{hp}$ [L/min]

$f_3(\bar{x}) = \Delta M_x$ [Nm]

$f_4(\bar{x}) = \Delta M_y$ [Nm]

$f_5(\bar{x}) = \overline{Mx}$ [Nm]

The design methodology in this study makes it very easy to add additional objective functions extremely quickly. It is extremely important to understand that the full optimization problem statement includes minimizing for all operating conditions. This is a theoretical problem statement; in reality the operating conditions must be sampled in order to characterize the entire space. It will be discussed in section 4.1.4 how the operating conditions are sampled in order to minimize the amount of simulations needed.

4.1.3 Constraints

This optimization problem also includes both types of constraints. These constraints have been implemented in order to allow the optimization algorithm to determine if a current design is realistic. This in optimization defined all designs that satisfy the constraint functions, feasible designs. A feasible valve plate would be a valve plate that could be safely installed and used with in the displacement unit. These constraints also allow the optimization algorithm to determine if the pressure module did not solve correctly.

4.1.3.1 Inequality Constraint(s)

There are five inequality constraints. Before explaining the constraints all the constraint functions are summarized first. All the inequality constraints are each bounded by a separate limit variable L. These limit variables are set in the beginning and remain constant throughout the running of the optimization algorithm.

$$g_1(\bar{\boldsymbol{x}}) = \text{Max pressure} \leq L_{max}$$

$$g_2(\bar{\boldsymbol{x}}) = \text{Min pressure} \geq L_{min}$$

$$g_3(\bar{\boldsymbol{x}}) = \text{Volumetric Efficiency*} \geq L_{voleff}$$

$$g_4(\bar{\boldsymbol{x}}) = \text{Max}(\left|\text{HP mean} - \text{set}\right|) \leq L_{hpmean}$$

$$g_5(\bar{\boldsymbol{x}}) = \text{Min}(\left|\text{LP mean} - \text{set}\right|) \leq L_{lpmean}$$

4.1.3.1.1 Pressure Extrema (Peak test)

In order to show all the operating conditions in a single figure a new type of plot has been introduced to. This plot is in short referred to as all Opcon plots. These plots will later be explained in section 4.1.4. For a single valve plate design, a very fine grid of operating conditions is simulated. All of the 1800s simulations are combined into a single graph. Multiple Opcon plots are then created to show multiple performance parameters. Figure 4.1 shows the maximum displacement chamber pressure, within one revolution and is normalized to the set high pressure values. For example, the highest point in the graph (left) is at operating condition 50 bar, 20% displacement, and 3400 rpm has maximum pressure of around 63 bar.

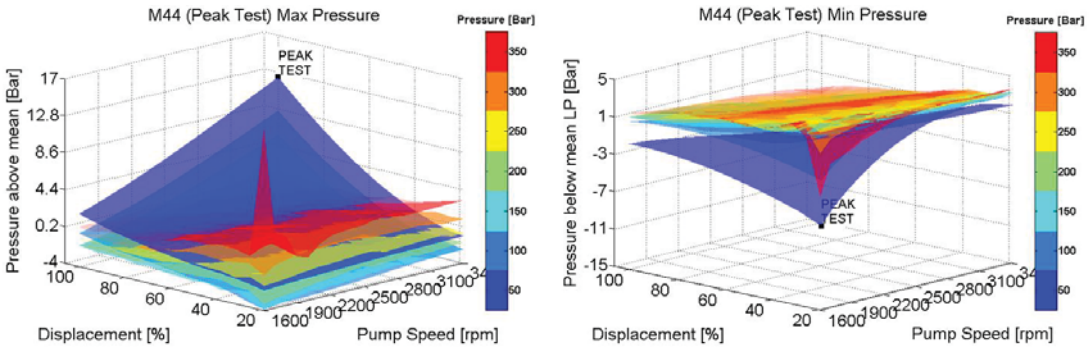

Figure 4.1. All Opcons Plots Maximum and Minimum Pressures.

In fact, both the largest maximum pressure and minimum pressure above/below average port pressures always occur at the same operating condition. This operating condition, as mentioned before, is the highest speed, highest displacement angle, and lowest Δpressure. Recall Eq. (3.20), the dv/dt term of the pressure buildup equation is the only term that can create pressures in the displacement chamber that are not between the port pressures. The dv/dt term increases with speed and displacement. The orifice flows to/from the ports will always help bring the pressure in the displacement chamber to the same as the corresponding port. These orifice flows always help reduce pressure peaks above/below the port pressures. These orifice flows are based on the differential pressure Eq. (3.22) and therefore minimized at the lowest high pressure. The pressure extrema will always be the worst at this operating condition. The inequality constraint check for pressure extrema needs only be done at this operating condition.

The reason to check for the maximum and minimum pressures of all the operating conditions is to ensure a safe operation of the pump. If the maximum pressure were to spike much greater than the original design, it could cause the pump to fail due to such large forces not previously considered by the original pump designers. The minimum pressure is checked to ensure no cavitation occurs within the pump.

4.1.3.1.2 Volumetric Efficiency*

Similar to the pressure extrema, the volumetric efficiency* (Section 3.7.3) always has a minimum. At the same operating condition. The operating condition is the lowest

speed, lowest displacement, and highest Δpressure. The volumetric efficiency*'s minimum always occurs at this operating condition because of cross porting.

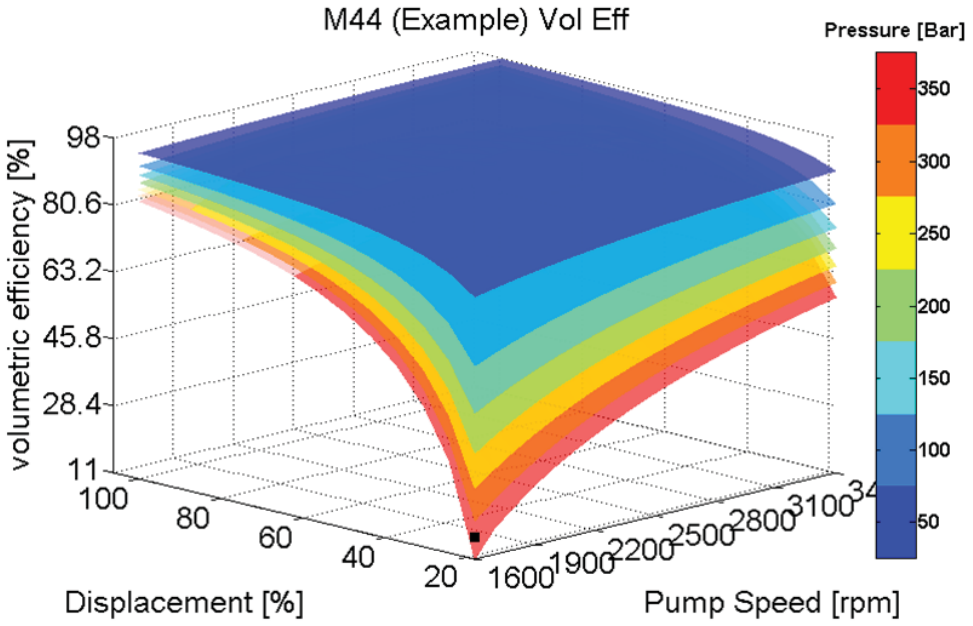

Figure 4.2. Opcon plot: volumetric efficiency*.

At the lowest speed and the highest pressure the cross porting is the greatest. The low speed allows a larger period of time to occur while cross porting. This allows more flow to occur. The high pressures also allow greater flows through the orifice areas located though relief grooves on the valve plate. While the leakage* is greater at high displacements, the leakage* percentage of the total discharge flow is greater at low displacements, because the total discharge flow reduces much more than the leakage*.

The volumetric efficiency* constraint is used in a different manner than previously. Volumetric efficiency* is already considered as an objective function. The volumetric efficiency* constraint was created to prevent the optimization algorithm from crashing. The optimization algorithm will decrease the volumetric efficiency* in order to decrease the other objective functions. Therefore, the volumetric efficiencies* would drop below 0% and eventually would always crash the pressure module software. In order to prevent the pressure module software from crashing, the volumetric efficiency* is set to be at least some small value, roughly 5%.

4.1.3.1.3 Set Pressures

The two set pressure inequality constraints were merely added to ensure the valve plate designs were indeed feasible in building pressure correctly. The optimization algorithm would choose valve plate designs that did not allow the displacement chamber to properly build up pressure to the set high pressure. Similarly, the optimization algorithm would choose valve plates that did not let the pressure drop all the way down to the set low pressure. In order to guarantee the valve plates were performing properly an inequality constraint was developed. These two inequality constraints simply check if the average high/low pressure is within some small tolerance of the set high/low pressure.

$$g_4(\bar{x}) = \max_{Opcons} \frac{|hp_{mean} - hp_{set}|}{hp_{set}} \leq L_{set} \tag{4.5}$$

Similarly, the low pressure was checked.

$$g_5(\bar{x}) = \max_{Opcons} \frac{|lp_{mean} - lp_{set}|}{lp_{set}} \leq L_{set} \tag{4.6}$$

4.1.3.2 Equality Constraint(s)

There is one equality constraint and it is also to ensure the valve plate designs are feasible and/or simulated correctly.

$$h_1(\bar{\boldsymbol{x}}) = \text{Finished Simulation} = L_{set} = \#\text{Opcons}$$

In order to make the pressure module more robust, the solver was implemented with an auto exit function when the solver found it very difficult to solve the system of equations. This prevents the pressure module from being stuck in infinite loops. There can also be other programming reasons why the pressure module could fail during its simulations. If the pressure module fails to finish the set amount of revolutions the performance parameters are still calculated. This encourages valve plate designs that force the auto exit function to have better performance parameters. For example, if the pressure module auto-exits before the pressure is built in the displacement chamber, the moments and flow ripples would be very small because the pressures were never properly

reached. (This would also fail the set pressure constraints). This constraint simply counts the number of revolutions completed and compares that to the number of revolutions set. If they are the same Boolean variable is set to 1. After every operating condition is simulated, they are summed. If a valve plate had any of its operating conditions fail to finish it fails this constraint and is not considered feasible.

$$h_1(\bar{x}) = \sum_{i=1}^{\#\ Opcons} \begin{matrix} 1, Completed \\ 0, \quad else \end{matrix} = \#Opcons\ Simulated \tag{4.7}$$

4.1.4 Operating Condition Sampling

The operating conditions in which the constraints are taken are now known. The next question to answer is what operating conditions are to be sampled in order to estimate the whole operating range for the objective functions.

From research done by Klop, 2010, it was shown that the noise generated by pump/motor is roughly proportional to the power transmitted. Therefore, the first operating condition to consider is the maximum power. Later explained in section 4.4, the maximum power can either be the maximum possible power of the unit or of the specific application. The next question follows is the maximum power operating condition sufficient to estimate the entire operating range. In order to answer that, the all Opcon plots were created and studied.

A review of section 2.3 will reveal that previous researchers have also tried to develop methodologies for estimating the entire operating condition space by sampling only a select number of operating conditions. The most successful sampling would be to safely characterize all of the solution space with the least amount of operating conditions simulated.

The amount of operating conditions is very influential on the total time needed to evaluate each valve plate design. The time needed is simply linearly proportional to the number of operating conditions simulated. Contrastingly, objective functions and constraints can easily be added with only negligible increases and computational time. Objective functions and constraints will only increase the time if it requires an additional operating condition to be simulated.

In the past, little was known about how the designs affected the entire operating condition space. In order to fill the void of understanding, a graphical way of presenting all of the operating conditions in a single image was developed. These operating condition plots (All Opcon plots) have led to a greater understanding of how the valve plate designs affect all the operating conditions. These plots have enabled sampling of the operating condition in a much more efficient and effective way than previously proposed methods.

In this study, ΔMx is used as the example performance parameter because it is most influenced by the operating conditions. The opaque section of the graph is the application specific operating conditions and the transparent section is the possible operating conditions for the pump. Labeled "OPCON A" is the maximum power (application) operating condition.

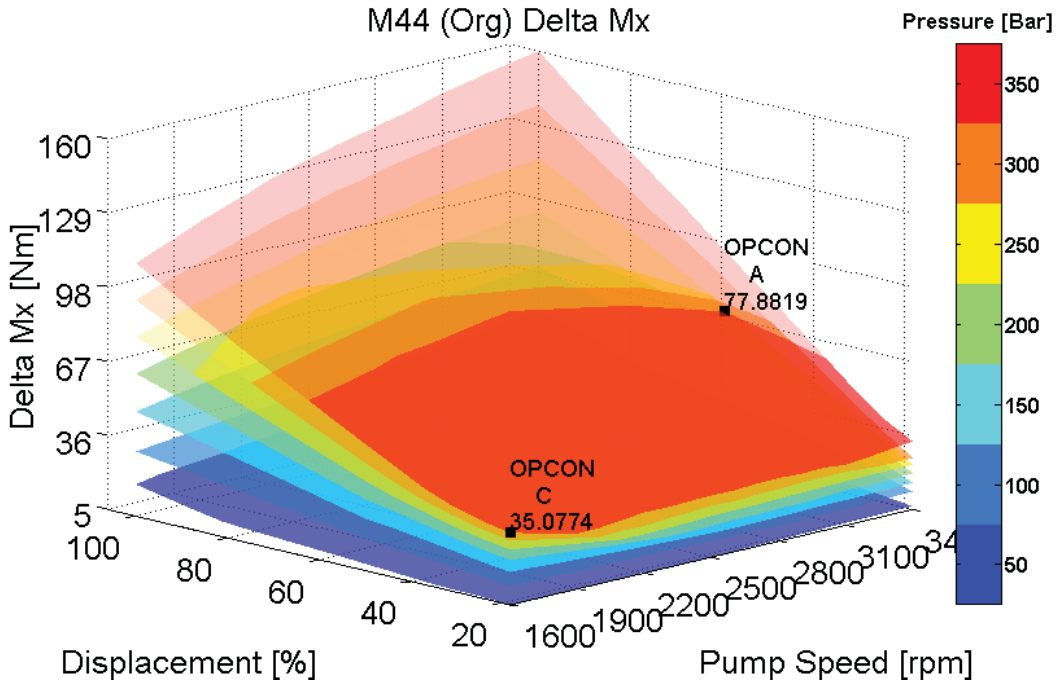

Figure 4.3. All Opcon plot: Original ΔMx.

The maximum power operating condition was then optimize in order to minimize the ΔMx. As can be seen in Figure 4.4, minimizing the maximum power operating condition (OPCON A) had a negative effect on other operating conditions. For example,

the low speed operating conditions increased from their original values in Figure 4.3. All Opcon plot: Original ΔMx

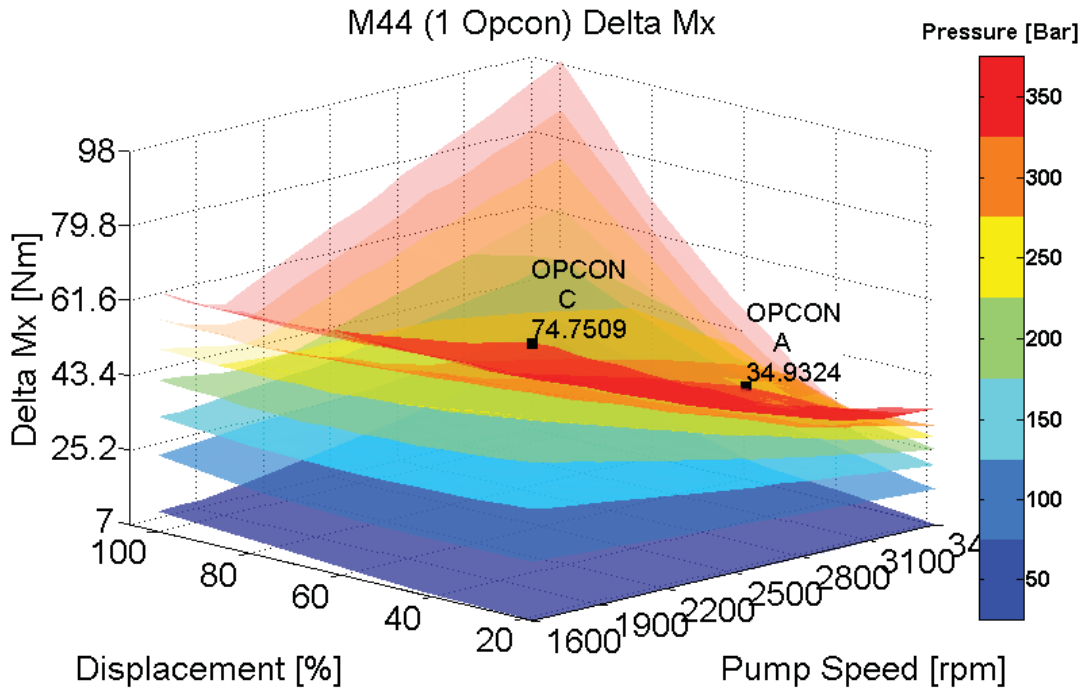

Figure 4.4. All Opcon plot: ΔMx; 1 Opcon sampled.

In order to prevent such a problem from occurring, another operating condition must be chosen. An obvious choice would have been 1600 rpm, 100 %, 350 bar. Choosing this operating condition would require a total of 4 operating conditions to be simulated. In order to minimize the total operating conditions simulated, the volumetric efficiency* constraint operating condition (OPCON C) was chosen because it is already needed to be simulated. A total of 3 operating conditions are needed in order to control the entire operating condition space.

The optimization was rerun using 2 operating conditions for evaluating the objective functions (ΔMx) and a balance of the two operating conditions was chosen. The results are shown in Figure 4.5. All Opcon plot: ΔMx; 2 Opcons sampled Compare Figure 4.5 with Figure 4.3 and it can be easily seen that the tested optimization algorithm could reduce the objective functions for the entire operating condition space using only 2 sampled operating conditions (3 with constraint).

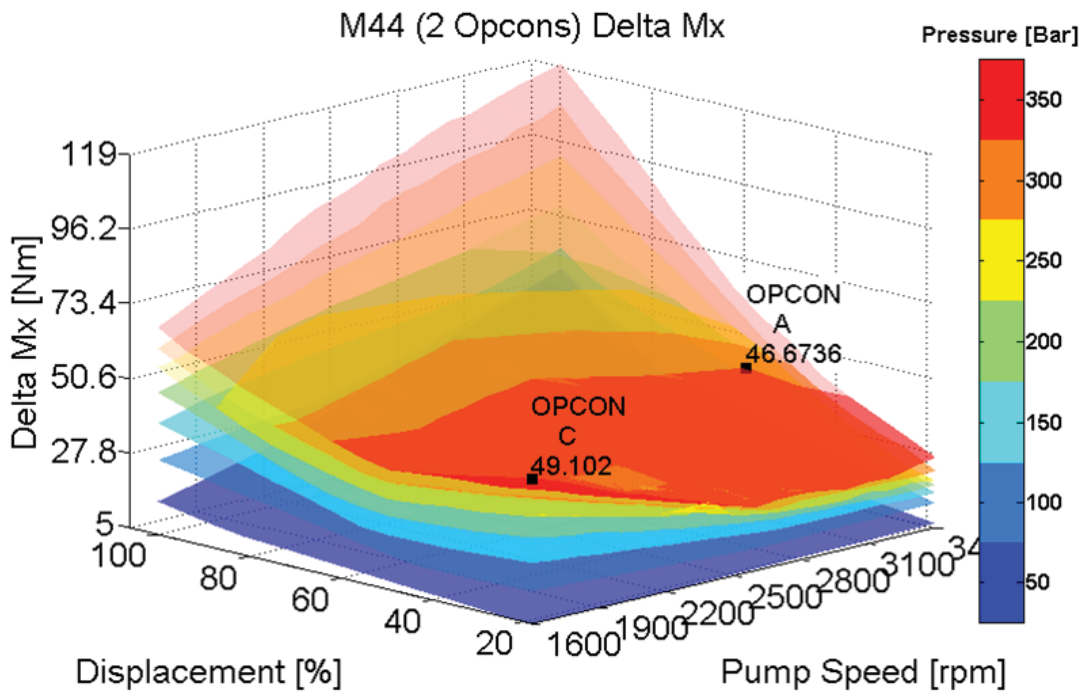

Figure 4.5. All Opcon plot: ΔMx; 2 Opcons sampled.

The use of the Opcon plots enables the designer to visualize the effects of how the sampled operating conditions affect the entire operating condition space. This allows the designer to simulate various small amounts of operating conditions during the optimization.

4.1.5 Problem Statement Summary

To summarize the valve plate design problem statement: there are five objective functions and six constraint functions simulated at the 3 different operating conditions, labeled below.

A. Maximum Unit Power (Application)

B. max n, min Δp, max β

C. min n, max Δp, min β

Different sets of data are used from the 3 operating conditions. The specific objective functions and constraints taken from each simulated operating condition are shown in Table 4.1. The combination of the 5 performance parameters and the 3 operating conditions creates eight total objective functions used in the optimization algorithm.

Table 4.1. Problem statement summary.

	A	B	C
Leakage* [%]			1
ΔQ_{hp}	2		6
ΔM_x	3		7
ΔM_y	4		8
$\overline{Mx}$	5		
Max pressure		*	
Min pressure		*	
Leakage*			*
$\lvert HP\ mean - set \rvert$	*	*	*
$\lvert LP\ mean - set \rvert$	*	*	*
Finished Simulation	*	*	*

4.2 Optimization Algorithm Selection

There is an enormous amount of research in the field of optimization. More specifically, there is a large amount of effort in the scientific community to develop optimization algorithms. Instead of developing another optimization algorithm specific to valve plate design, the focus on this research study was on gaining a better understanding of the fundamental principles behind the various existing optimization algorithms and chose an algorithm that is fitting to the specific problem. The three main characteristics of the valve plate design optimization problem consist of: multi-objective optimization, global optimization, and parallelization. These three characteristics yield a specific set of optimization algorithms that would be very successful in solving the given problem.

4.2.1 Multiobjective Optimization

As previously mentioned, the successful design of a valve plate requires the minimization of multiple performance parameters. This belongs to a class of optimization termed multiobjective optimization. Multiobjective optimization problem consists of reducing a vector of multiple objective functions into a scalar which is a single objective function. In the end, all optimization algorithms need a single scalar in order to quantify the quality of an individual design. There are numerous methods for solving the multi-objective problem.

The state-of-the-art in noise reduction of axial piston machines does not fully understand the relationship between structure borne noise sources and fluid borne noise sources. Moreover, different hydraulic systems powered by the same pump will require different priorities for structure borne noise sources and fluid borne noise sources. These facts make it very hard for the designer to know the relative importance/priority to give to the various objective functions.

The most intuitive solution to a multi-objective problem is the weighted average approach. This involves assigning a coefficient to each objective function and summing all the weighted objective function values to a single weighted average. This approach was used in Kim, 2012 and requires the designer to know the weights A priori or simulate all the variations of weights. However, there are more efficient, sophisticated ways of solving the multi-objective problem

4.2.1.1 Pareto Optimal

Within a multiobjective problem, design A can only be certainly better then design B, if design A has all of its objective function values smaller, then all of design B's objective function values. This is defined as A dominates B.

The set of all designs that are not strictly dominated by any other design are termed non-dominated designs. Non-dominated designs are also referred to as Pareto optimal. The set of all Pareto optimal designs form the Pareto front. The Pareto optimal designs are all the designs that can be clearly stated as better than all the non-Pareto optimal designs. Therefore, given any number of objective functions and priorities the best design will always be Pareto optimal.

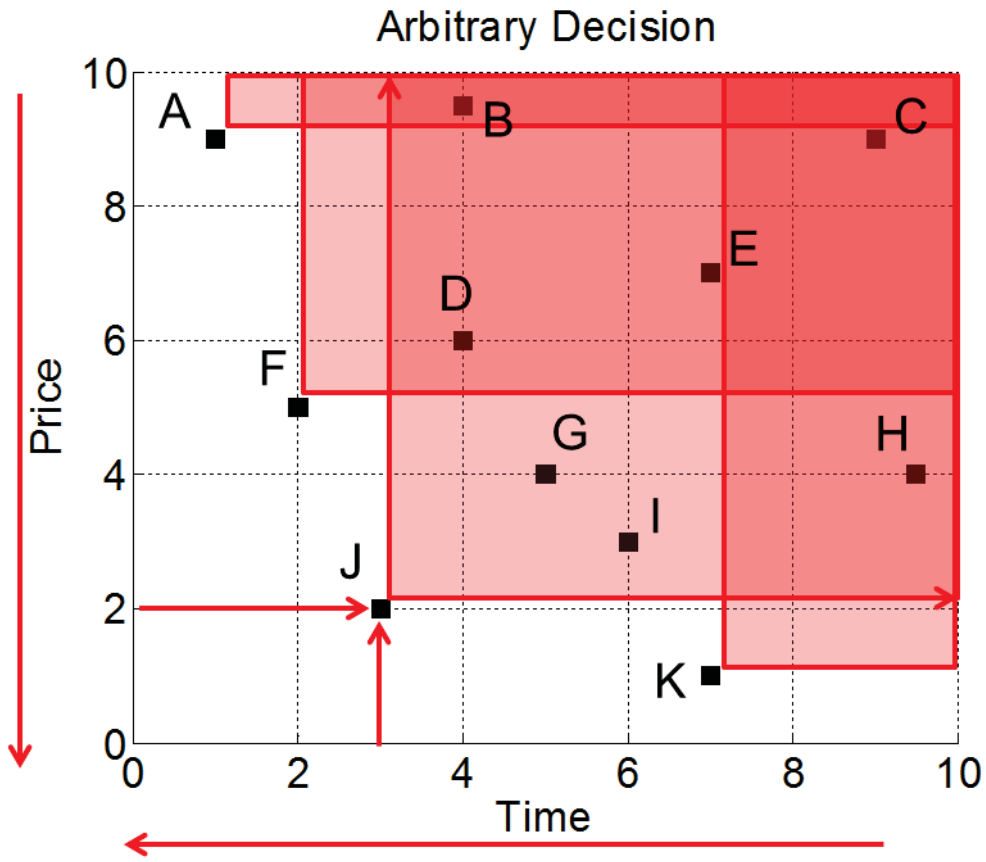

Figure 4.6. Simple multi-objective example.

Figure 4.6 shows a very classic example of a Pareto front. The Multiobjective optimization problem consists of minimizing both production time and the selling price of a product. For this particular product, decreasing the production time could potentially increase the cost of the product. Design J is better at both time and price than then designs B,D,G,I,H,E,C. Therefore, design J dominates all of those designs. Design J is clearly better in both time and price, then all of those designs.

Now compare designs J and K. Design J is better in time but not in price as compared to design K. Both designs J and K are Pareto optimal designs because no design dominates J or K. Within the Pareto front, improving one objective function is always accompanied by worsening a different objective function. Therefore, moving throughout the Pareto front is a subjective preference made by the designer.

A real Pareto front from a famous multiobjective optimization problem is shown below. Another important term to define is the utopian point. The utopian point is not a

real design and is the perfect solution to the multiobjective problem. The creation of the utopian point is done by taking the smallest value from every objective function independently along the Pareto front and creating a single utopian point. The utopian point is very useful to understand how small each objective function can possibly become.

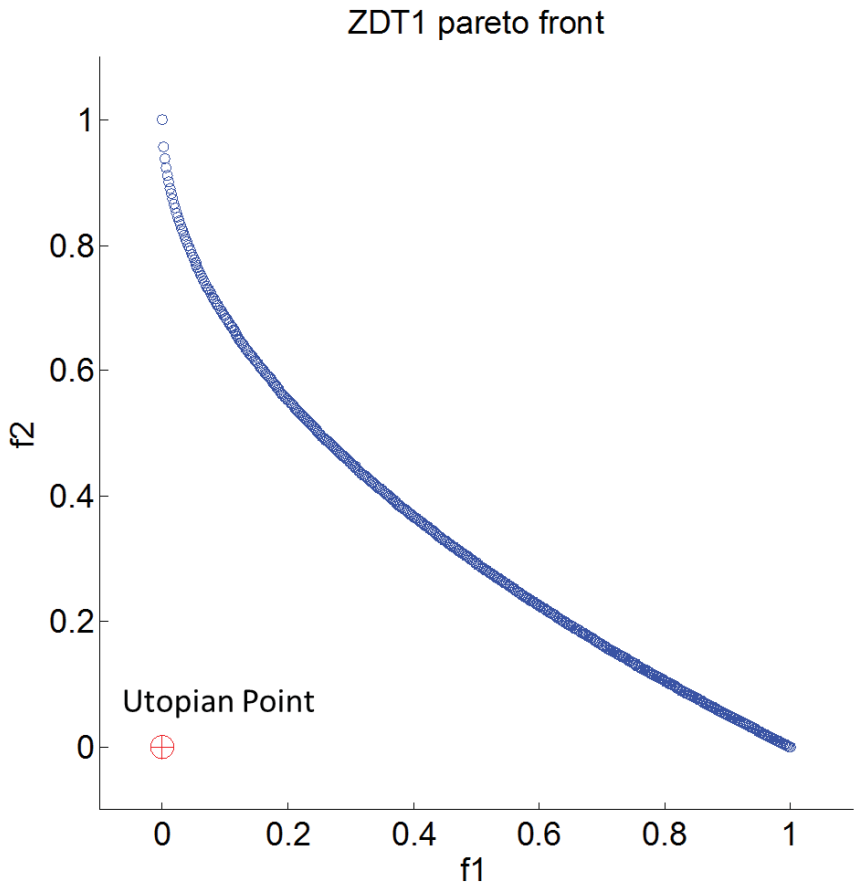

Figure 4.7. ZDT1 Pareto Front.

Many Pareto front examples are shown curved, but realize a line drawn between the points (0,1) and (1,0) would also be a Pareto front. To better understand the concept of Pareto optimal designs and Pareto front's, another example of a three-dimensional and therefore three objective functions Pareto front is shown below.

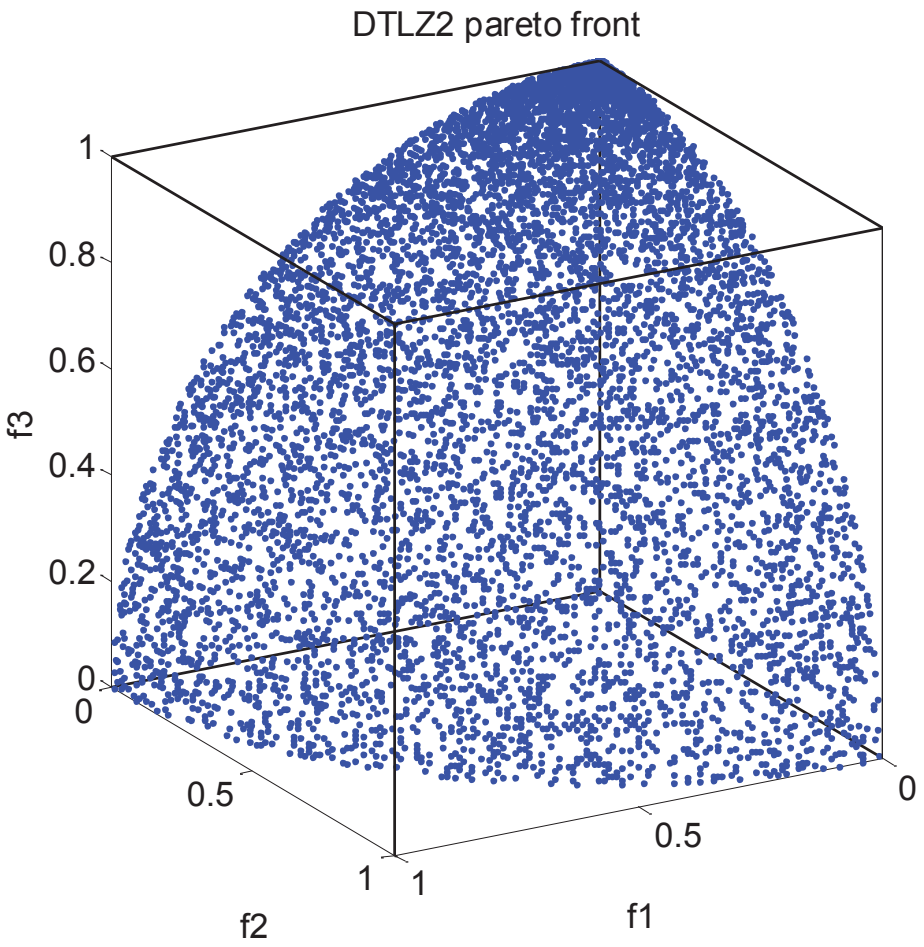

Figure 4.8. DTLZ2 Pareto Front.

This Pareto front was created using a classical optimization problem, DTLZ2, which tries to maximize the objective functions.

Optimization algorithms based on the principle of Pareto optimality are well-suited for the valve plate design problem because the relative priorities of the various operating conditions are not known before the optimization algorithm is simulated. There are several optimization algorithms developed in order to build the Pareto front. The most popular algorithm being non-dominated sorting.

4.2.1.2 Non-dominated Sorting

Non-dominated sorting was first developed in 1995 (Srinivas & Deb, 1995) as a way of solving the multiobjective optimization problem. Non-dominating sorting was later improved in Deb, 2002 by implementing a faster sorting algorithm. Non-dominating sorting algorithm is based on calculating how many designs in a population dominate each design. This calculation defines the rank of each design. Once the rank is known for every design, the designs are simply sorted using the non-domination rank. Referring to Figure 4.6, Table 4.2 records the non-domination ranks of all the designs in the simple multi-objective example.

Table 4.2. Example Domination Rank.

Domination Rank	Points (Designs)
0 (Pareto)	A,F,J,K
1	G,I
2	D
3	B,H
4	E
5	C

The non-domination rank is simply a more generalized concept and Pareto optimality, in that Pareto optimal is one special class of non-domination ranks. This very simple yet elegant solution to the Multiobjective problem as shown to be extremely robust and efficient. Non-dominating sorting is based on comparing a group of designs and therefore can only be used with population-based algorithms (Figure 2.1)

4.2.2 Global Optimization

Global optimization is a branch of optimization that is distinguished from regular optimization by the fact that it focuses on finding the global minimum (or maxima) in not just local minima (or maxima). Any optimization problem can be phrased as a global optimization problem, but in general global optimization problems consist of a solution space that contains many local minima (extrema). Among the numerous local extrema, there exists a single global extrema.

A famous global optimization benchmark problem is shown below. As can be seen from Figure 4.9 and the corresponding contour plot underneath the surface, there are many local minimum.

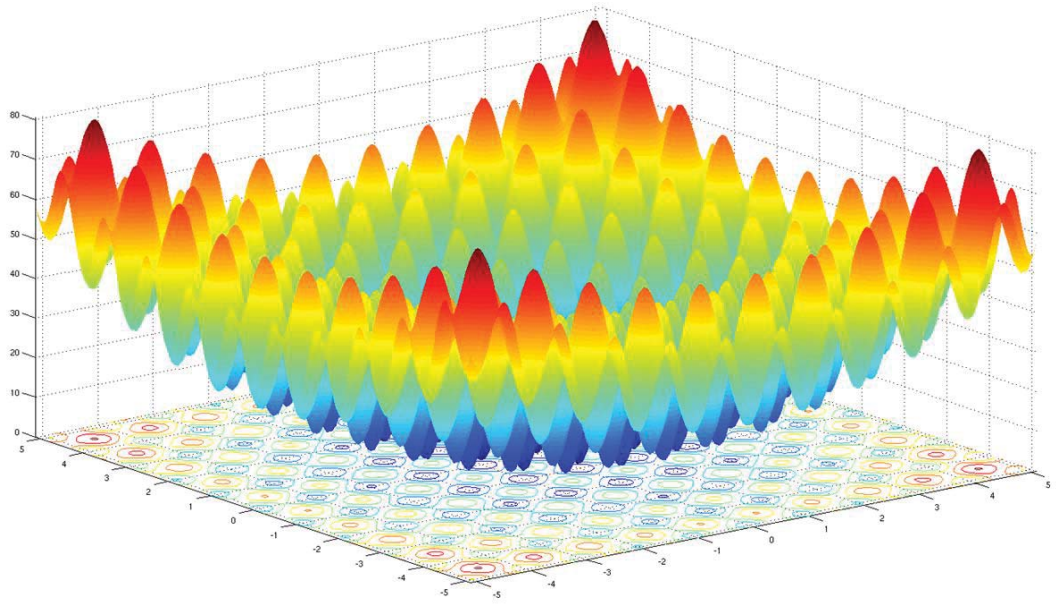

Figure 4.9. Rastrigin's Function.

The Rastrigin function was developed to test multiobjective optimization algorithms and was designed to be difficult to solve. The function describing the Rastrigin function is shown below.

$$f(\bar{x}) = A_n + \sum_{i=1}^{n} {x_i}^2 - Acos(2\pi x_i) \tag{4.8}$$

,where A = 10 and $-5.12 \leq X_i \leq 5.12$. It has a global minimum at x = 0 where f(x) = 0

The selected optimization algorithm needs to be robust enough to be able to solve the global optimization problem. From previous observations, it was seen that some objective functions are much easier to minimize than others. This observation in essence causes previous tested optimization algorithms to converge to a local minima instead of finding the global minimum. This was also apparent when the same optimization algorithm would converge to different local minimum when iterated through multiple simulations.

The fact that the valve plate design must be treated as a global optimization problem immediately excludes most of the classical optimization routines. Most of the classical optimization routines are unable to "climb out" of a local minimum and converge too quickly to a sub-optimal solution.

4.2.3 Parallelization

As previously discussed in section 3.8, the logic within the pressure module contains large amounts of concurrency and therefore makes the simulations of multiple valve plates over multiple operating conditions very easy to be parallelized. This parallelization greatly increases the simulation speed of the pressure module.

Similarly, it is important for computational time that the selected optimization algorithm contains similar concurrent sees and is able to take advantage of the parallelization of simulations.

Within the field of optimization algorithms, the two main quantities of an algorithm that quantifies its performance are: the number of function evaluations in the final solution found (smallest amount). Typically, an algorithm that can build a Pareto front that is closest to the real Pareto front (with known Pareto front) with the least amount of function evaluations is considered the most successful. However, in real world applications the total wall clock time is more important than total function evaluations. Algorithms that utilize parallel computing may have slightly greater function evaluations, but substantially less simulation times because of the parallelism.

One notable example of a Multiobjective optimization algorithm that builds the Pareto front would be the MOEA/D (Zhang & Li, 2007) algorithm. However, this

algorithm cannot be parallelized trivially and therefore was not selected as a potential candidate for solving the valve plate optimization problem.

4.2.4 Selected Algorithm: NSGA-II

Nondominated sorting genetic algorithm II (NSGA-II) is the selected optimization to solve the valve plate optimization problem (VpOptim). NSGA-II satisfies all the necessary constraints given by the valve plate design problem. A complete explanation of the algorithm is given by its creators (Deb, Pratap, Agarwal, & Meyarivan, 2002) so it is not necessary to explain all the fine details of the algorithm. In summary, NSGA-II satisfies the following necessities:

1. Can solve multiobjective optimization problems
    a. Uses non-dominated sorting
    b. Creates evenly distributed Pareto front
2. Can solve global optimization problems
    a. Utilizes a genetic algorithm
    b. Is not calculus-based
3. Can be parallelized
    a. Is population-based

NSGA-II also has the ability to solve constrained optimization problems and utilizes elitism to improve the performance of the genetic algorithm. One final and very important characteristic that the NSGA-II algorithm satisfies is the availability of the source code. NSGA-II and other algorithms developed by Deb and his colleagues release the source codes freely to the general public. This allows researchers to easily utilize their research without spending hundreds of hours programming their algorithms. This algorithm is implemented in Matlab and sub-functions have been created to communicate the information between the global algorithm and all the parallelized pressure modules running on multiple machines.

4.3 Design Methodology Overview

All the various components of the entire design methodology have been individually explained. The entire design methodology can now be properly explained. The following flowchart summarizes the entire proposed design process in this thesis, including the implementation of the selected optimization algorithm (NSGA-II).

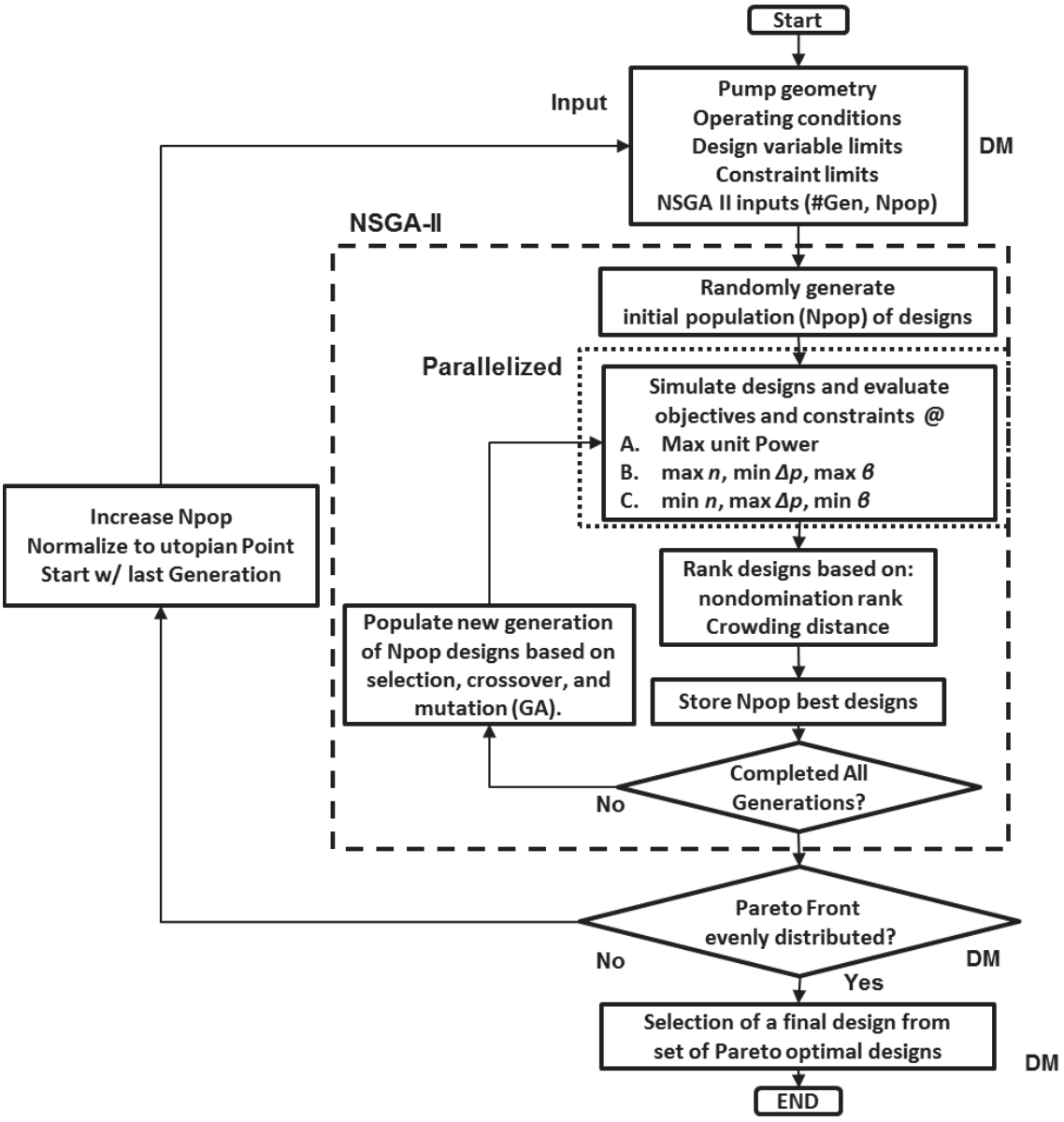

Figure 4.10. Proposed design methodology.

4.3.1 Pre-NSGA-II

Before starting the NSGA-II algorithm, the designer must first specify the following inputs needed for the pressure module and/or the optimization algorithm. One subtle improvement to the valve plate design methodology is reducing the number of inputs needed to be supplied by the designer. This simplifies the design process, but also reduces the total design time needed as each input requires additional time by the designer. The following lists of inputs are required by the pressure module and are not design variables and therefore remain constant throughout the entire design process. Only the three **bold inputs** are information not readily available to the public. However, the bold inputs can be measured if the designer has access to an existing pump. This allows vehicle manufacturers to design valve plates for their machines without requiring technical information from the supplier.

1. Specify Oil bulk modulus and viscosity (function of pressure and temperature)
2. **Pitch Diameter Cylinder Block**
3. **Diameter Piston**
4. Max Swash Plate Angle
5. Number of Pistons
6. **Displacement chamber dead volume**

Secondly, the designer will need to choose the operating conditions specific to their application. If the designer has no experience with which operating conditions to choose, the three operating conditions (A, B, and C) will satisfy the majority of valve plate designs.

The design variable limits and constraint limits given in the following case study will provide a guideline. The design variable limits given in the case study are designed to increase the variable boundaries as far as possible. It is therefore highly recommended to use the predetermined variable limits. Decreasing the variable limits were only decrease the possible access of the optimization and increasing the variable limits will most likely cause logical errors within the program. The constraint limits given in the following case study are also designed to be very conservative. The constraint limits were also designed

to be very general and have worked with multiple pump sizes and operating condition ranges.

Finally, the two NSGA-II variables; number of generations and population size are typically two very difficult variables to know a priori. However, the proposed new design methodology enables the designer to change these variables at the end of the optimization algorithm without having to rerun the entire optimization.

It is recommended that the number of generations be set to a high number (200 to 300) because both stop and pause buttons have been implemented allowing the designer to stop NSGA-II, at any generation.

It is recommended that the designer increase the population size to at least 100 times the number of objective functions. Using the standard eight objective functions would require a minimum of 800 as a population size. The important factor to consider when choosing the population size is sufficiently estimating the Pareto front with enough discrete designs. The final Pareto front will have Npop number of designs.

4.3.2 NSGA-II

The best improvement of by the current design methodology is the ability of the optimization algorithm to completely automate the optimization once the NSGA-II has begun. Previous design methodologies required decisions to be made by the designer throughout the optimization process. This would create barriers in the optimization algorithm that required the algorithm to wait all night, or all weekend until the designer comes back to work and makes the decision. These implicit waiting functions are neglected in the published simulation times by Seeniraj and Kim.

The NSGA-II will run for the given set number of generations and the given population size. The simulation time for a single generation will be very consistent. It is therefore recommended that the designer utilize extra time during the nights and weekends to run more generations.

4.3.3 Post-NSGA-II

The output of the NSGA-II is the set of all Pareto optimal designs of size Npop. Therefore, a single valve plate design must be chosen by the designer from the final Pareto optimal designs. This final decision made by the designer is the most abstract decision throughout the entire design methodology. This choice will be based on the designer's priorities of the objective functions. This can be based on the specific application, measurement results, cost analysis, client preferences, and manufacturing abilities (of the valve plates). For this reason not a lot of advice can recommended on how to choose the final valve plate design. However, a safe choice from the Pareto optimal designs would include all designs that strictly dominate the original valve plate design. This will guarantee the chosen valve plate has better performance parameters than the original design.

4.3.4 Evenly Distributed Pareto Front

One final decision made by the designer shown in the algorithms flowchart is the evenly distributed Pareto front. This decision may be obvious to some, but for the sake of completion it is shown in the methodology. What if the final Pareto front, given by the NSGA-II algorithm, does not contain designs close to a specific set of design priorities (objective function weights). For example, the final Pareto front could contain large areas between designs where the designer would wish to choose a design from.

The flowchart gives two recommendations in order to encourage NSGA-II to output a specific desired design performance. Increasing the population size will create a more discrete approximation of the Pareto front. Normalizing to the utopian point will help the algorithm distribute designs more evenly along the Pareto front.

After updating the population size and normalizing to the utopian point, the designer does not need to start the optimization algorithm from the beginning. The designer can simply start the optimization algorithm, giving the last population as an initial condition (initial population). If the population size was increased part of the population will be Pareto optimal, the remainder of the initial population will be randomly generated. The optimization algorithm can then begin where it left off and

genetic algorithm can quickly generate more designs along the Pareto front within a few generations.

4.4 Application Specific Optimization

The proposed current design methodology is an extremely fast design process as compared to the state-of-the-art in valve plate design. This design methodology enables the designer to have a large amount of control over the preferred objective functions. This design methodology's high level of control and speed enables a designer to quickly design, for the same pump, different valve plates, depending on the application. The same displacement unit could be used in multiple machines that require different priorities of the performance parameters. For example, the same pump could be installed in:

1. A car where noise is very important (specifically structure borne noise sources) in the control moment is important. The operating condition varies considerably.
2. A manufacturing facility, where the fluid borne noise sources are more important. The operating condition remains fairly constant.
3. A construction vehicle, where the control moment is very important and needs to be negative (tending towards minimal displacement)

Application specific valve plate design enables the pump manufacturer or an applications engineer to customize the same pump for a wider range of applications. To consider the design for various applications, the designer only needs to consider two components of the design methodology.

4.4.1 Opcon Sampling

The sampling of the operating conditions for each specific application allows the designer narrow the optimization to only consider the usable, operating range of that application (machine). As previously explained (Figure 4.3 - Figure 4.5), minimizing a single, operating condition will cause negative consequences on other operating conditions. Therefore, when minimizing multiple operating conditions, a compromise must be made. Decreasing the operating conditions based to be more specific to the application decreases the amount of compromise needed. A smaller range of operating

conditions will allow the designer to improve the performance parameters to greater amounts.

4.4.2 Pareto Front "Weights"

The second component of the design methodology that changes with different applications is a selection of the specific Pareto optimal design within the Pareto front. Different applications, as previously discussed, require different sets of priorities on the performance parameters. This design methodology makes it very convenient for the designer to choose different designs from the Pareto front if the different applications happen to operate with in the same range of operating conditions.

CHAPTER 5. CASE STUDY

The proposed new design methodology was tested using a 44 cc axial piston pump. The valve plate was done for a specific application where noise was the highest priority among the performance parameters. The following case study is organized by following the required steps outlined in Figure 4.10.

5.1 Simulation Setup

The pump geometry used in this case study is confidential and will not be shared. The design of the simulation setup prioritized simplicity without sacrificing generality. The individual pump and application only requires the changing of a few inputs. The following table reiterates the recommended lower bound an upper bound for all the design variables.

Table 5.1. Case study variable boundaries.

Variable	**Lower Bound**	**Upper Bound**	**Units**
e1	-15	-5	[deg]
e2	5	15	[deg]
e3	-15	-5	[deg]
e4	5	15	[deg]
l1	0	30	[deg]
l2	0	30	[deg]
l3	0	30	[deg]

Table 5.1. Continued.

l4	0	30	[deg]
r1	0	2	[mm^2]
r2	0	2	[mm^2]
r3	0	2	[mm^2]
r4	0	2	[mm^2]
x1	1	15	[unit less]
x2	1	15	[unit less]
x3	1	15	[unit less]
x4	1	15	[unit less]
m1	0.01	0.1	[mm^2/deg]
m2	0.01	0.1	[mm^2/deg]
m3	0.01	0.1	[mm^2/deg]
m4	0.01	0.1	[mm^2/deg]

In addition to the groove design variables, the pressure module requires the lower bound and upper bounds for the pre-compression and de-compression filter volumes. The upper boundary is equal to the lower boundary for the filter volumes. This simply guarantees the genetic algorithm will always use the same value. Notice the volume for the filter volume is very near zero. This essentially removes the filter volumes from the design.

Table 5.2. Case study filter volume boundaries.

Variable	**Lower Bound**	**Upper Bound**	**Units**
ϕ_{SPCFV}	0.22	0.22	[deg]
ϕ_{PCFV}	2	2	[deg]
m_{PCFV}	4	4	[mm^2/deg]

Table 5.2. Continued.

ϕ_{SDCFV}	0.22	0.22	[deg]
ϕ_{DCFV}	182	182	[deg]
m_{PCFV}	184	184	[mm^2/deg]
r_{PCFV}	0.0012	0.0012	[deg]
V_{PCFV}	9e-5	9e-5	[deg]

The operating conditions chosen were based on the recommendations given in CHAPTER 4. The specific values follow the recommendations and are based on the specific application used for the case study.

Table 5.3. Case study operating conditions.

OpCon	**Speed [rpm]**	**Displacement [%]**	**High Pressure [bar]**	**Low Pressure [Bar]**
A	3200	50	345	25
B	3400	100	50	25
C	1600	20	345	25

The constraint limits were also set as follows:

Inequality constraints:

$$g_1(\bar{x}) = \text{Max pressure} \leq 200 \text{ bar}$$

$$g_2(\bar{x}) = \text{Min pressure} \geq 10 \text{ bar}$$

$$g_3(\bar{x}) = \text{Volumetric Efficiency*} \geq 5\%$$

$$g_4(\bar{x}) = \text{Max}(|\text{HP mean} - \text{set}|) \leq 0.1 \text{ (10\% difference)}$$

$$g_5(\bar{x}) = \text{Min}(|\text{LP mean} - \text{set}|) \leq 0.2 \text{ (20\% difference)}$$

Equality constraint(s):

$$h_1(\vec{x}) = \text{Finished Simulation} = 3$$

The final two inputs needed were the NSGA-II inputs. The number of generations was set to 200. The population size (Npop) was set to 450. Simulation setup is now complete and the simulation can begin.

5.2 Simulation Statistics

Everything within the NSGA-II box (Figure 4.10) is performed automatically in the algorithm does not require the user to understand the inner workings of the optimization algorithm. The optimization algorithm continues simulation until all 200 generations are completed or when the user chooses to early terminate the program because the designs are acceptable.

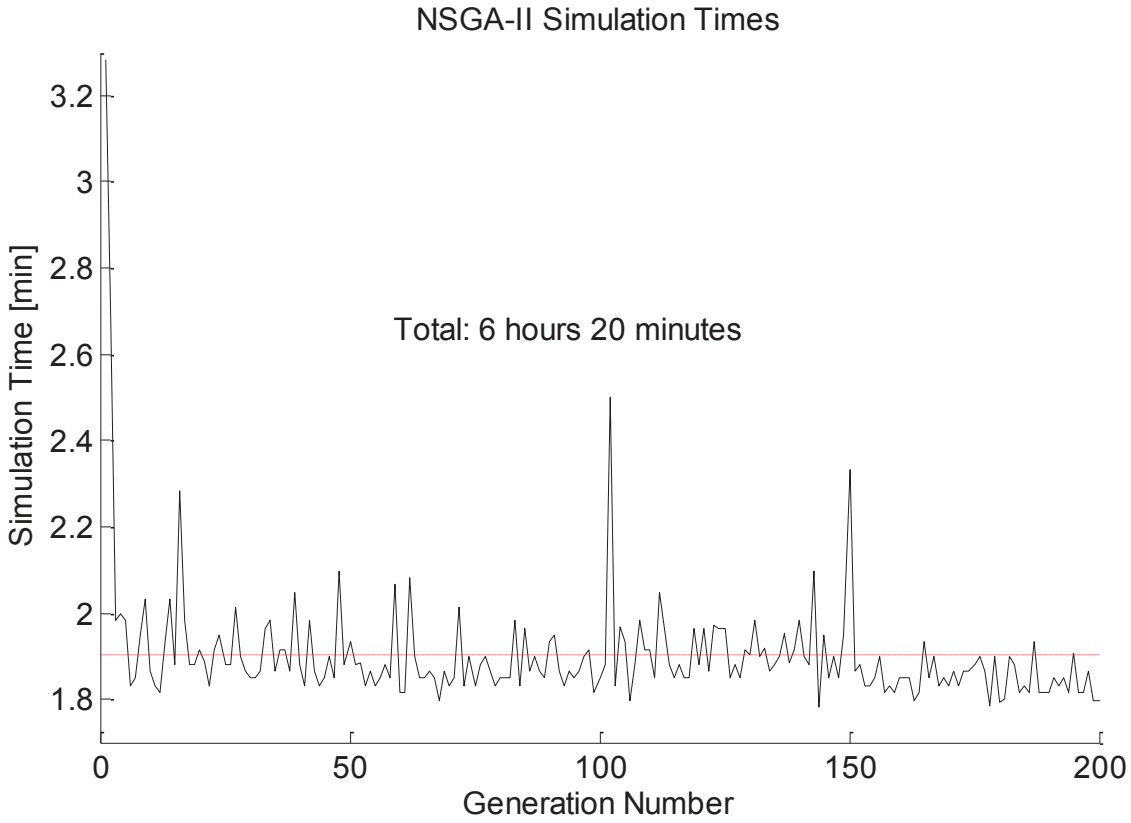

Figure 5.1. Case study simulation times.

The optimization algorithm utilizes parallelization on multiple computers. The total number of simultaneous simulations was 120 threads. Each valve plate took on average 30 seconds to complete a simulation. Figure 5.1 shows the total simulation time for each generation. The small variations in simulation time are mainly due to the variations in the designs parameters, each requiring different iterations of the LSODA solver. Notice the first generation is significantly higher than the rest because the first population is randomly generated, and contains a wider variety of designs and also worst designs which are harder for LSODA to solve. The total average simulation time per generation was roughly 1.9 minutes. The total simulation time was roughly 6 hours. The Pareto front generated by NSGA-II was sufficiently evenly distributed.

5.3 Results

The output of the NSGA-II simulations is a set of 450 (Npop) Pareto optimal designs. It is extremely difficult to graphically depict 450 designs, each containing 8 objective functions. Under a normal design process, the designer would select only one final design. For the purpose of education, three designs were selected in order to highlight the design methodology.

5.3.1 Radar Plots

Three Pareto optimal designs were chosen to highlight the possible noise reductions. The radar plot is a very convenient way of graphing more than three variables. Each axis of the radar plot (Figure 5.2. 8 objective functions Radar Plots) is used to plot a different objective function. Notice, each axis has a different scaling, as the different objective functions naturally have different ranges.

The original valve plate is shown in blue as a control. The best ΔM_{xA} was chosen to highlight the lowest possible ΔMX at operating condition A. Similarly, the best ΔQ_{hpA} was chosen to highlight the lowest possible flow ripple at operating condition. A. Notice for both these valve plate designs a huge compromise must be made in order to decrease a single objective function so drastically. All of the other objective functions (ΔQ_{hpA}) are worse than the original design for the ΔQ_{hpA} valve plate design. This highlights the multi-

objective nature of valve plate design in the consequences of neglecting some of the performance parameters.

The fourth and most important Pareto optimal design chosen would be a balance selection of all the objective functions.

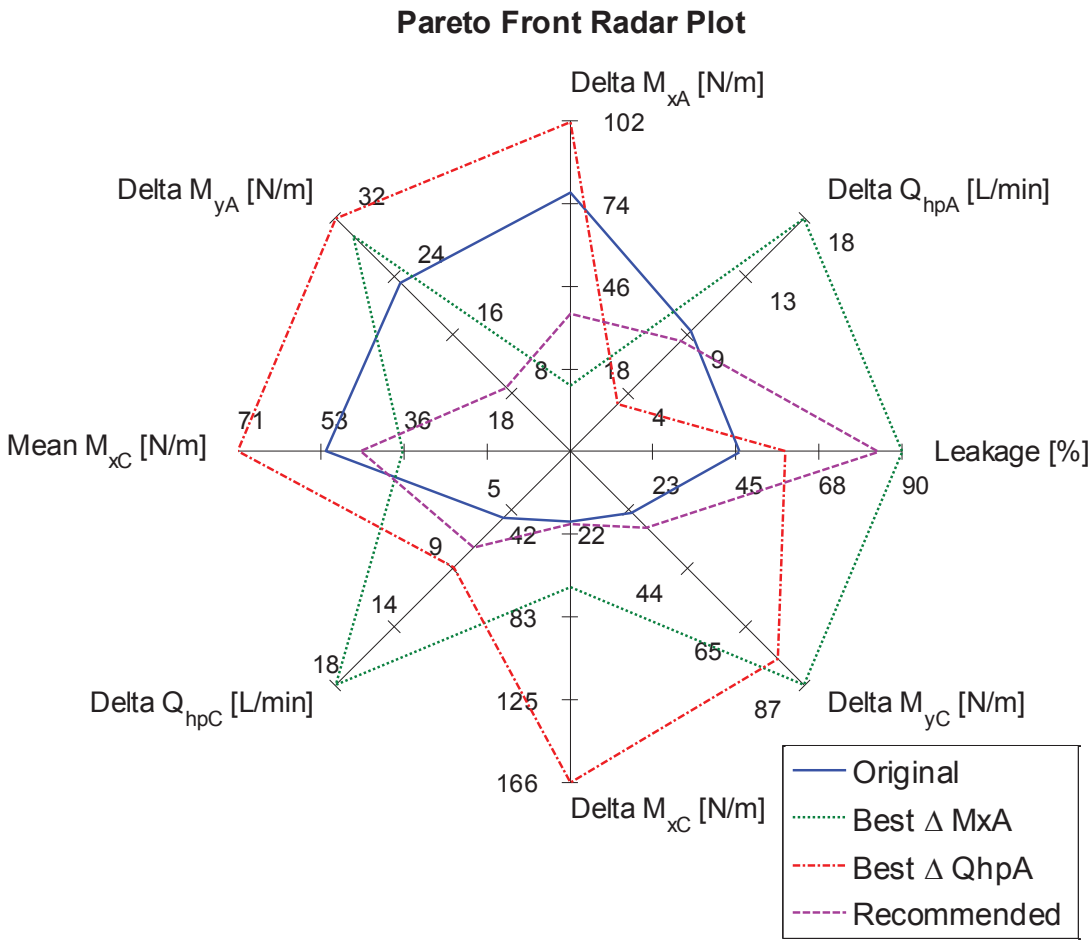

Figure 5.2. 8 objective functions Radar Plots.

The actual application did not require 3 of the objective functions to be important. The five important objective functions for this case study are shown separately. Notice the information in Figure 5.3 is the same as in Figure 5.2. This case study was designed to decrease the noise sources near operating condition A without sacrificing the original noise source levels at operating condition B.

Therefore notice in Figure 5.3, the recommended Pareto optimal valve plate design strictly dominates the original design in the performance parameters that were

considered important for the case study. The case studies design objectives was to minimize ΔM_{xA} without sacrificing ΔM_{xC}. This is apparent noticing the recommended valve plate's ΔM_{xC} is practically equal to the original valve plate's ΔM_{xC}.

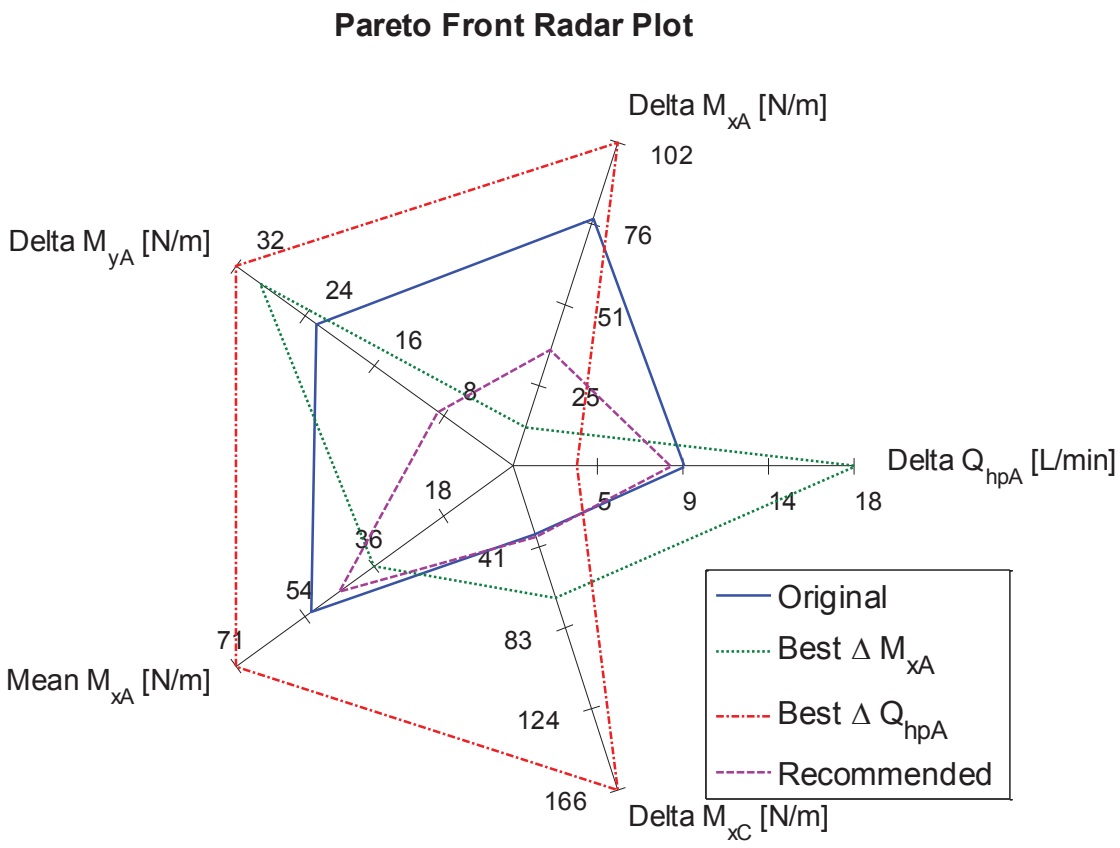

Figure 5.3. Important 5 objective functions Radar Plot.

5.4 Case Study Conclusions

The radar plots and Opcon plots are very useful to quickly qualitatively compare multiple designs. However, the precise quantitative comparison of the multiple designs is best done with the use of a table showing the actual numbers. Table 5.4 summarizes the eight objective function values for the four compared to designs. The numbers highlighted in green are the most important reasons each design was chosen.

Table 5.4. Case Study selected Pareto Designs.
Forward Pumping

Design	$Leakage_C$ [%]	ΔQ_{hpA} [L/min]	ΔM_{xA} [Nm]	ΔM_{yA} [Nm]	Mean M_{xA} [Nm]	ΔQ_{hpC} [L/min]	ΔM_{xC} [Nm]	ΔM_{yC} [Nm]
Original	46.0	9.2	77.6	23.1	-52.2	5.1	35.0	22.8
Best ΔM_{xA}	90.2	18.3	12.3	29.6	-35.7	18.2	67.9	86.6
Best ΔQ_{hpA}	58.4	3.5	101.6	32.5	-71.5	8.9	166.0	76.9
Recommended	83.3	8.4	36.8	8.7	-44.8	7.3	36.4	28.5

Similarly, Table 5.5 summarizes the percent reduction of each objective function as compared to the original design. Notice the "Best ΔM_{xA}" design drastically reduces the ΔM_{xA}, but also drastically increases most of the other objective functions. The "Best ΔQ_{hpA}" has an enormous ΔM_{xC}. These two designs could never be chosen for a real system and less for research purposes.

The recommended design was chosen because it reduces the most amounts of objective functions without having to compromise.

Table 5.5. Case Study Selected designs percent change.
Forward Pumping

Design	$Leakage_C$ [%]	ΔQ_{hpA} [L/min]	ΔM_{xA} [Nm]	ΔM_{yA} [Nm]	Mean M_{xA} [Nm]	ΔQ_{hpC} [L/min]	ΔM_{xC} [Nm]	ΔM_{yC} [Nm]
Original	0%	0%	0%	0%	0%	0%	0%	0%
Best ΔM_{xA}	96%	99%	-84%	28%	-32%	259%	94%	280%
Best ΔQ_{hpA}	27%	-62%	31%	40%	37%	76%	374%	237%
Recommended	81%	-8%	-53%	-62%	-14%	45%	4%	25%

The overwhelming success of these results is hard to realize without the comparison of the previous design methodologies. Seeniraj, 2009 reduced the ΔM_x by roughly 10% and Kim, 2012 could not reduce the ΔM_x and increased on average 13%. This reduction of 53% is a very significant reduction.

This case study reveals the proposed design methodologies ability to efficiently optimize all the performance parameters to the limitations of the physics. The design

methodology excessively populated the entire eighth dimension Pareto front allowing the designer to simply choose the desired priorities of performance parameters.

CHAPTER 6. CONCLUSIONS

The main topic of this thesis was to develop a design methodology for improving the performance of valve plates in the most general way possible. The computational model used was previously developed and verified to be an accurate prediction of the valve plate's performance parameters. A new differential equations solver was implemented and demonstrated an increased simulation speed by 100 times without sacrificing accuracy.

The design methodology was developed for designers that did not have intricate knowledge of how the valve plate affects the performance of the pump. The use of an optimization algorithm allows a non-technical user to optimize a valve plate without the gears of experience needed prior.

Table 6.1 highlights the major similarities and differences between the current design methodology proposed and its predecessors. The main improvements center on the vast improvements to automation and speed.

Table 6.1. Design Methodology Overview.

	Seeniraj	**Kim**	**Kalbfleisch**
Opcon #	8	3	3
Peak test	Yes	Yes	Yes
Vol eff*	No	Yes	Yes
Finish all sims check	No	No	Yes
Set pressures check	No	No	Yes
1 design sim time	16.2 mins*	15min/thread	30 sec/thread

Table 6.1. Continued.

Design of experiments	Full factorial	Full factorial	NSGA-II
Multi Objective	Human	Single** Weighted avg	Pareto Front
Parallelization	No	One variable	Yes
Function evaluations	292,736	370,000	Set: 90,000
Total Optimization time	300 hours (11 weeks)	Not documented	6 hours
Human involvement	In loop	In loop	Not In loop

*: Estimated

**: Implemented Improperly

A great amount of effort was taken to ensure both the pressure module simulations in the optimization algorithm were robust enough to handle as many of the possible errors that can occur numerically in the models. An Auto exit function was instrumented in the pressure module to prevent infinite loops. Additional constraints were added to the optimization algorithm in order to ensure feasible valve plates were being simulated. These additional constraints automate the design process and allow the algorithm to continue without the need of the designer making decisions.

The improvements to speed consist of a 100 times speed up from the LSODA differential equations solver, in 140 times speed up from the parallelization, and a subtle 8/3 speed up by reducing the number of operating conditions needed to estimate the entire operating condition space. This creates a combined speed up in simulation time of roughly 37,000 times. The parallelization architecture allows the speed up to increase linearly with the amount of computers available. Utilizing more computers will enable even greater amounts of speed improvements.

The improvements to speed and to the optimization algorithm in reducing the amount of function evaluations needed have allowed greater complexity of designs. The complexity of the valve plate designs has been increased from six design variables for the

grooves to 20 design variables. This increase in complexity allows the optimization algorithm the freedom to find significantly better designs than previously allowed.

A case study was done in order to highlight the performance of the design methodology. The case study involved an existing stock axial piston pump optimized for the application of a real working machine. The case study highlights the success of the design methodology to optimize the valve plate quickly and efficiently. The design methodology does not only optimize the valve plate for specific component (displacement unit), but also takes into account the specific application (vehicle). The case study shows the success of the design methodology in substantially improving the performance parameters of a valve plate design.

LIST OF REFERENCES

LIST OF REFERENCES

Becker, R. J. (1970). Quieting Hydraulic Systems and Components. *Society of Automotive Engineers. Combined National Farm, Construction & Industrial Machinery and Powerplant meetings.* Milwaukee, Wisconsin.

Blum, C., & Roli, A. (2003). Metaheuristics in combinatorial optimization: Overview and conceptual comparison. *ACM Computing Surveys*, 268-308.

Dawkins, R. (1976). *The selfish gene.* NewYork: Oxford University Press.

Deb, K., Pratap, A., Agarwal, S., & Meyarivan, T. (2002, April). A fast and elitist Multiobjective genetic Algorithm: NSGA-II. *IEEE transactions on evolutionary Computation, 6*(2).

Dréo, J. (2007, September 26). *Metaheuristics classification fr.svg*. Retrieved from http://commons.wikimedia.org/wiki/File:Metaheuristics_classification_fr.svg

Edge, K. A. (1999). Designing quieter hydraulic systems - some recent developments and contributions. *Fourth JHPS International Symposium on Fluid Power*, (pp. 3-27). Tokyo, Japan.

Edge, K. A., & Liu, Y. (1989). Reduction of piston pump pressure ripple. *Second International Conference on Fluid Power Transmission and Control.* China.

Ehrgott, M. (2012). Vilfredo Pareto and Multi-objective Optimization. *Journal der Deutschen Mathematiker-Vereiningung, Extra Volume 21st ISMP*, 447-453.

Eldredge, N. (1989). *Macro-evolutionary dynamics: species, niches and adaptive peaks.* NewYork: McGraw-Hill.

Goldberg, D. E. (1989). *Genetic algorithms for search, optimization, and machine learning.* Reading, MA: Addison-Wesley.

Harrison, A. M. (1997). *Reduction of axial piston pump pressure ripples.* PhD Thesis, University of Bath, UK.

Helgestad, B. O., Foster , K., & Bannister, F. K. (1974). Pressure transient in an axial piston hydraulic pump. *Institution of Mechanical Engineers*, (pp. 189-199).

Hindmarsh, A. C. (1983). ODEPACK, A Systematized Collection of ODE Solvers. *IMACS Transactions on Scientific Computation, 1*, 55-64.

Holland, J. H. (1975). *Adaptation in natural and artificial systems.* Ann Arbor, MI: University of Michigan Press.

International Organization for Standardization. (1983). *Hydraulic fluid power -- Pumps, motors and integral transmissions -- Parameter definitions and letter symbols* (Vol. ISO 4391:1983).

Ivantysn, J., & Ivantysynova, M. (2001). *Hydrostatic Pumps and Motor, Principles, Designs, Performance, Modeling, Analysis, Control and Testing.* New Delhi: Academic Books International.

Ivantysynova, M., Huang, C., & Christiansen, S. K. (2004). Computer Aided Valve Plate Design - An Effective Way to Reduce Noise. *Proceedings of the SAE Commercial Vehicle Engineering Congress & Exhibition.* Chicago, IL USA: SAE Technical Paper.

Johansson, A. (2005). *Design Principles for Noise reduction in Hydraulic Piston Pumps - Simulation, Optmization and Experimental verification.* PhD Thesis, Linkoping University, Sweden.

Kim, D. (2012). *Contribution to digital prototyping of axial piston pumps/motors.* MS Thesis, Purdue University.

Kim, T., Kalbfleisch, P., & Ivantysynova, M. (2014). The effect of cross porting on derived displacement volume. *International Journal of fluid power, 15*(2), 77-85.

Klop, R. J. (2010). *Investigation of Hydraulic transmisson Noise Sources.* PhD thesis, Purdue University.

Li, H. (2009, 05 22). *Solving Stiff ODEs*. Retrieved from sourceforge.net: http://lh3lh3.users.sourceforge.net/solveode.shtml

Osman, I. H. (1993). Metastrategy simulated annealing and tabu search algorithms for the vehicle routing. *Annals of Operations Research*, 41:421-451.

Palmberg, J. O. (1989). Modelling of flow ripple from fluid power piston pumps. *2nd Bath International Power Workshop.* Univeristy of Bath, UK.

Pettersson, M., Weddfelt, K., & Palmberg , J. O. (1991). Methods of reducing flow ripple from fluid power piston pumps - a theoretical approach. *SAE International Off-highway and Powerplant Congress.* Milwaukee, USA.

Petzold, L. (1983, March). Automatic Selection of methods for solving stiff and nonstiff systems of ordinary differential equations. *SIAM Journal on Scientific and Statistical Computing, 4*(1).

Seeniraj, G. K. (2009). *Model based optimization of axial piston machines focusing on noise and efficiency.* PhD Thesis, Purdue University.

Srinivas, N., & Deb, K. (1995). Muiltiobjective Optimization Using Nondominated Sorting in Genetic Algorithms. *Evolutionary Computation, 2*(3), 221-248.

Tiwari, S., Fadel, G., & Deb, K. (2011). AMGA2: improving the performance of the archive-based micro-genetic algorithm for multi-objective optimization. *Engineering Optimization*, 377-401. doi:10.1080/0305215X.2010.491549

Wieczorek, U., & Ivatysynova, M. (2002). Computer aided optimization of bearing and sealing gaps in hydrostatic machines - the simulation tool CASPAR. *International Journal of Fluid Power, 3*(1), 7-20.

Yamauchi, K., & Yamamoto, T. (1976). Noises gernated by hraulic pumps and their control method. *Mitsubshi techical review, 13*(1).

Zecchi, M. (2013). *A novel fluid structure interaction and thermal model to predict the cylinder block/valve plate interface performance in swash plate type axial piston machines.* PhD Thesis, Purdue University.

Zhang, Q., & Li, H. (2007). MOEA/D: A Multiobjective Evolutionary Algorithm Based on Decomposition. *Evolutionary Computation, IEEE Transactions*, 712-731.

LIST OF PUBLICATIONS

LIST OF PUBLICATIONS

Kalbfleisch, P. (2012). Noise Reduction in Hydraulic axial-piston pumps and motors. *Machine Dynamics and Vibro Acoustics.* Samara, Russia: Samara State Aerospace University.

Kim, T., Kalbfleisch, P., & Ivantysynova, M. (2014). The effect of cross porting on derived displacement volume. *International Journal of fluid power, 15*(2), 77-85.